

**Thesis submitted in partial fulfillment of the requirement for the
degree of Master of Bioprocess Engineering**

on

**Development of fruit-waste derived bio-
adsorbent for removal of
pharmaceutical contaminant from
aqueous solution**

by

SOUMITRA MALLIK

Class Roll No: 002110303012

Exam Roll No M4BPE23006

Registration no 160024 of 2021-2022

Under the guidance of

(Prof.) Dr. Mehabub Rahaman

&

(Prof.) Dr. Saswata Bose

DEPARTMENT OF CHEMICAL ENGINEERING

JADAVPUR UNIVERSITY

Kolkata - 700032

SELF DECLARATION OF CREATIVITY OF ACADEMIC PRINCIPLES

I hereby confirmed that the thesis work contains on the basis of a literature survey and original research work by the undersigned candidate, as part of “The **Master of Engineering in Bioprocess Engineering** studies. All information in this document has been obtained and presented in accordance with academic rules and ethical conduct

Name : Soumitra Mallik

Exam Roll no. M4BPE23006

Registration no 160024 of 2021-2022

Project Title: Development of fruit-waste derived bio-adsorbent for removal of pharmaceutical contaminant from aqueous solution

Signature :

Date :

CERTIFICATION

This is to certify that Mr.Soumitra Mallik, a final year student in the Master of Bioprocess Engineering examination in the Department of Chemical Engineering, Jadavpur University, bearing Registration No: 160024 of 2021-2022 has successfully completed the thesis work entitled **“Development of fruit-waste derived bio-adsorbent for removal of pharmaceutical contaminant from aqueous solution”** under the guidance of **(Prof.) Dr. Mehabub Rahaman** and **(Prof.) Dr. Saswata Bose** during master degree curriculum. This work has not been reported earlier anywhere and can be approved for submission in partial fulfillment of the requirements for the Master of Engineering in Bioprocess Engineering.

(Prof.) Dr. Mehabub Rahaman

Supervisor
Department of Chemical Engineering
Jadavpur University

(Prof.) Dr. Saswata Bose

Co-supervisor
Department of Chemical Engineering
Jadavpur University

(Prof.) Dr. Rajat Chakraborty

Head of the Department
Department of Chemical Engineering
Jadavpur University

Dean

Faculty of Engineering & Technology
Jadavpur University

CERTIFICATE OF APPROVAL

This thesis is hereby approved as the creditable study of an engineering subject carried out and presented in a manner satisfactory to warrant its acceptance as a prerequisite to the degree for which it has been submitted. It is understood by this approval that the undersigned don't approve any statement made, opinion expressed or conclusion drawn therein but approve the thesis only for the purpose of which it is submitted.

(Prof.) Dr. Mehabub Rahaman

**Supervisor
Department of Chemical
Engineering
Jadavpur University**

(Prof.) Dr. Saswata Bose

**Co-supervisor
Department of Chemical
Engineering
Jadavpur University**

Signature of the Examiners

ABSTRACT

In this work, a low-cost adsorbent from abundantly available biowaste jamun seed (*Syzygium cumini*) was developed via carbonization and chemical-activation process. It was utilized to remove one of the pharmaceutical drug, ofloxacin, from its aqueous solution. The surface morphology and surface area of the prepared activated Jamun seed dust were investigated by “Field Emission Scanning electron microscope” (FESEM), “Brunauer-Emmet-Teller”(BET), “Fourier Transform Infrared Spectroscopy” (FTIR), particle size analysis. The surface area of Activated Jamunseed (ACJS) was found as 366.39 m²/g. The carbon content of Jamun seed powder was found after CHNS analysis is 55.68 %.The removal rate of Ofloxacin from aqueous solution by activated Jamun seed powder (ACJS) was 96% at 3.5 hr, maintaining pH of the solution is 5. The highest adsorption capacity of ACJS was 39.97 mg/g. The adsorption kinetics followed linear pseudo-2nd-order model with R²=0.9999. The isotherm study has shown that Langmuir linear isotherm fitted with experimental data.From the thermodynamics study indicates the adsorption is feasible and exothermic process.The activated carbon which is derived from Jamun seed powder, also cost effective and can be utilized upto five cycles without compromising the removal efficiency of OFC from aqueous solution.

ACKNOWLEDGEMENT

At first I would like to thank my respected guide **(Prof.) Dr. Mehebub Rahaman Sir**, and **(Prof.) Dr. Saswata Bose sir**, without their active guidance, valuable technical support, valuable advice, help as well as supervision I would not have been able to complete my project. I am very much grateful to my guide for providing me the golden opportunity to accomplish this project. I must thank everyone in the Chemical Engineering department for helping me with my project work.

I am very grateful to all laboratory technicians in the chemical engineering department, their sincere help has helped me to make my work easier to carry forward my project work.

I am very special gratitude towards the head of the department, (Prof.) Dr. Rajat Chakraborty and all the respected Professors of the Chemical Engineering department.

Finally I am very grateful to my guide as well as supervisor Prof. (Dr.) Mehebub Rahaman sir, and Prof. (Dr.) Saswata Bose sir for their continuous support, advice and help during the thesis work.

A special thank to my parents, and my friends.

Thanking You,

Soumitra Mallik

Registration no 160024 of 2021-2022

Exam Roll no. M4BPE23006

Bioprocess Engineering

Department of Chemical Engineering

MBPE 2nd year

CONTENTS

Self-declaration of creativity and conformity of academic principles.....	ii
Certification.....	iii
Certificate for approval.....	iv
Abstract.....	v
Acknowledgement.....	vi
Nomenclature, Abbreviations & List of Tables.....	ix
List of figures.....	x
Chapter 1.	
Introduction.....	2
1.1 Effects on aquatic environment of Ofloxacin.....	4
1.2 Background study.....	4
1.3 Purification technology of removal of Ofloxacin from wastewater.....	7
1.4 Activated carbon as the adsorbent.....	9
1.5 Objective.....	11
Chapter 2	
2.1 Required Material.....	13
2.2 Preparation of activated Carbon	13
2.3 Characterization	14
2.4 Particle size analyzer	17
2.5 Batch Adsorption studies	17
2.6 The adsorption isotherms.....	19
2.7 Studies on adsorption Kinetics.....	21
2.8 Intra-particle diffusion model.....	22
2.9 Studies on adsorption thermodynamics	23
2.10 Regeneration study.....	24

Chapter 3 Result and Discussion

3.1 Characterization	26
3.1.1 Proximate and Elemental analysis.....	26
3.1.2 SEM –EDS analysis.....	26
3.1.3 FTIR analysis.....	28
3.1.4 BET analysis.....	30
3.1.5 Particle Size analysis.....	31
3.2 Batch adsorption studies.....	32
3.2.1 Effect of ratio of KOH and CJS with time.....	32
3.2.2 Effect of solution pH.....	33
3.2.3 Effect of adsorbent dosages.....	34
3.2.4 Impact of initial concentration of Ofloxacin.....	35
3.2.5 Effect on Temperature.....	39
3.3 . Isotherm studies	37
3.4 Kinetic Studies on Adsorption.....	43
3.5 Thermodynamics study on adsorption.....	46
3.6 Regeneration study	49

Chapter 4

4 Conclusion

Chapter 5

5 References

Nomenclature

<i>Symbols</i>	<i>Description</i>
C_i	Initial concentration
C_o	Final Concentration after removal
Re	Removal efficiency
T	Temperature
Q_t	Adsorption Capacity at time t

Abbreviations

<i>Initialism</i>	<i>Description</i>
AC	Activated carbon
OFC	Ofloxacin
JS	Jamun seed
ACJS	Activated Jamun seed
PJS	pyrolyzedJamun seed
API	Active pharmaceutical ingredient
BET	Brunauer-Emmet-Teller
SEM	Scanning Electron Microscope
CHNS	Carbon Hydrogen Nitrogen Sulphur analysis
FTIR	Fourier Transform Infrared Spectroscopy

List of Tables

Table.1	Introduction of Ofloxacin.....	3
Table.2	Effect of Ofloxacin onenvironment.....	4
Table.3	Represents the CHNS data of PJS and JS.....	26
Table.4	Experimental results on various adsorption isotherm.....	38
Table.5	Results on adsorption kinetic model.....	43
Table.6	Represents the Thermodynamics studies.....	48

List of Figures

Figure.1	Structure of Ofloxacin.....	3
Figure.2	Experimental steps to prepare ACJS from jamun seed (JS).....	15
Figure.3	Standard plot to determine the concentration of OFC in aqueous solution.....	19
Figure.4	SEM morphology of (a) JS and (b) ACJS.....	28
Figure.5	EDS spectrum of ACJS.....	28
Figure.6	FTIR spectrum of (a) JS and (b) ACJS.....	30
Figure.7	Hyteresis loop of ACJS in BET.....	32
Figure.8	Particle size distribution of ACJS.....	32
Figure.9	Effect ratio of KOH and CJS of adsorbents.....	33
Figure.10	Effect of pH of solution.....	35
Figure.11	Effect of ACJS dosage on removal of OFC.....	36
Figure.12	(a). Effect of initial concentration of OFC on removal efficiency of ACJS.....	37
	(b). Adsorbent capacity vs removal percentage of OFC.....	37
Figure.13	Effect of temperature on the removal of OFC.....	38
Figure.14	(a). Langmuir linear adsorption isotherm plot.....	40
	(b). Nonlinear Langmuir Isotherm plot.....	41
Figure.15	(a). Linear Freundlich adsorption isotherm model.....	42
	(b). Non linear Freundlich adsorption isotherm model.....	42
Figure.16	Temkin adsorption isotherm.....	43
Figure.17	(a).Linear pseudo 1 st order kinetics.....	45
	(b). Linear pseudo 2 nd order kinetics.....	46
Figure.18	Intraparticle diffusion model.....	47
Figure.19	Thermodynamic study on adsorption of OFC.....	48
Figure.20	Determination of activation energy on adsorption.....	49
Figure.21	Regeneration of ACJS.....	50

CHAPTER 1

INTRODUCTION

1.Introduction

Nowadays one of the most emerging contaminants for the environmental eco-system is pharmaceutical drugs, which are exerted from human urine, expired medicine, hospitals, industrial effluent etc. Because of excessive use of medication for different purposes not only by human lives but also for agricultural purposes, fish farming, veterinary medicine, etc. which increases the buildup of large amounts of pharmaceutical drugs in wastewater[1]. Different categories of pharmaceutical residue are identified for uses of human livestock in the environment, such as antibiotics, steroids, non-steroids, narcotic analgesics, inhalants, etc. Some of these are highly water soluble, low degradable, and mixed with groundwater (drinking water) levels through natural filtration, which causes different health issues for not only the aquatic ecosystem but also other parts of the environment.

Among these pharmaceuticals, antibiotics are largely used in human livestock, and they are the main source of pharmaceutical pollutants coming from hospital waste, expired medicine, and pharmaceutical effluents[2,3]. Pharmaceutical effluent releases a large amount of active pharmaceutical ingredients (API) of antibiotics. Among the API of antibiotics, few are easily dissolved in water, few were partly soluble or insoluble. Some antibiotics increase the resistance of bacterial pathogens, some of them are very toxic to algae and have harmful effects[4,5]. Sometimes antibiotic does not decrease health proficiency, and physiological changes but also enhances bacterial health resistance[6,7]. Antibiotics also help recompense mutation of microorganisms and reimburse their physical fitness[8]. It is very sad to say, negligence of improper management and their carelessness upon discarding the residue of API of antibiotics into the ecosphere, including aquatic ecosystems, surface, and seawater, which causes serious health issues due to non-degradable nature. Some non-degradable API can possess their stability in sewage treatment, conventional activated sludge process which performs in the removal stage[9,10]. Subsequently, these contaminants enlarge into the environment by several processes.

Among them, Ofloxacin (OFC) is one of the antibiotics which is largely used. It is a type of antibiotic in the fluorinated quinolones group[11]. Ofloxacin is a second-generation antibiotic [12]. A racemic mixture of OFC contains 50 % lev-Ofloxacin and 50% of enantiomer of dextr-Ofloxacin. The (-) isomer is approximately to a greater extent of 10-100 times enough influential than the (+) isomer against gram (+) and gram (-) bacteria for antimicrobial activity[13]. Ofloxacin is not able to be entirely metabolized through a physical body and it is

mostly exerted through the urine and then dumped into the drainage system in hospitals or cities. OFC decreased the amount of Chlorophyll in the ecosystem, which causes the microscopic population's capacity for photosynthetic processes may have decreased[14,15]. In addition, the wastewater treatment plant failed to entirely remove OFC. Water from the surface, the soil, and the slit can be affected by the residual OFC in the wastewater treatment plant sewage[16]. The natural balance of watery ecosystems and microbes may be threatened by the continual addition of antimicrobial drugs. Cyanobacteria are the aquatic creatures that are most prone to fluoroquinolones because of their similarities in structure to microorganisms. After being exposed to OFC, the prokaryotic community's morphology altered, and its level of difficulty also decreased considerably. This suggests that OFC may have an impact on the prokaryotic communal ability to survive and may upset the balance of the ecosystem.

OFC uses for various purposes like eye drops, ear drops, (Oflox, Oflop,) and tablet like Zancin 200, "O₂" for bacterial infections of various organs such as urinary tract, nose infections, pneumonia, diarrhea, and lower respiratory problem. OFC released from human urine is 80% and remains unchanged.[17]

Bio-degradability is an important factor to decompose antibiotic drugs, in STP but biodegradation of OFC is very poor[18]. If an excess amount of Ofloxacin consumed in the body is higher than the permissible limit, then it may affect serious health problems like abdominal pain, chest pain, anxiety, fever, skin rash, constipation, etc. An excessive dosage of OFC can cause permanent nerve damage serious nervousness, agitation, etc. Thus removal of OFC from wastewater is very important. The physical properties and effect of OFC on the environment are shown below[19].

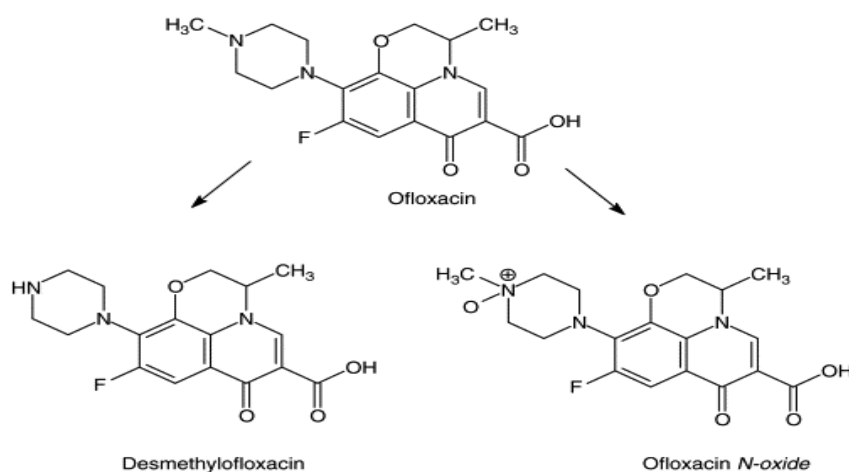


Figure 1 Structure of Ofloxacin

Table 1: Properties of Ofloxacin

IUPAC name	((RS)-7-9-fluoro-2,3-dihydro-3-methyl-10-(4-methyl-1-piperazinyl)-7-oxo-7H-pyrido[1,2,3-de]-1,4-benzoxazine-6-carboxylic acid)
Molecular weight	361.388
Molecular formula	C ₁₈ H ₂₀ FN ₃ O ₄
Melting point	254°C
Solubility	Soluble in aqueous solution between pH 2 to pH 5. Sparingly soluble in aqueous solution with pH 7.

Table 2: Effects of Ofloxacin on environment

Genotoxicity	1-2 µg/l
susceptible pathogens	7.5 µg/l
Excretion rate (unchanged in the environment)	70%
Concentration in hospital wastewater	50 µg/l, 1088 µg/l, [20]
During drug production	853 ng/l
Animal culture	4ng/l
Sewage wastage	123 µg/l
Pharmaceutical wastage	150-160 µg/l [21]
Industrial influent	373 /day[22]

1.2 Literature survey

Liu et. al. [23] removed OFC through the degradation process by a Fenton-like system using Fe₃O₄-CeO₂/AC. The ratio of Fe and AC is 1: 3 by weight and Ce and AC is 0.54:1 by weight. The percentage of degradation OFC is at pH 3.3 and initial OFC conc. was 12 mg/l and catalyst 0.5g/l. In this process, much, more chemical is used like FeSO₄·7H₂O, H₂O₂ HCL, HCOOH, and H₂SO₄, NH₄OH, Cerium (III) nitrate hexahydrate, N-Butanol, and KI. The process is very much expensive to carried out.

Ahmed and Imam[24] developed a degradation process by the Fenton method using a composite of Fe_3O_4 Montmorillonite. In this process they used $\text{FeCl}_3 \cdot 6\text{H}_2\text{O}$, $\text{FeSO}_4 \cdot 7\text{H}_2\text{O}$, HCL , NH_4OH , Montmorillonite, H_2O_2 . Here adsorbent doses 0.75g/l Fe - Montmorillonite, and the percentage of degradation was about 81 at neutral medium within 120 min in the dark condition.

E. Hapeshi et al.[12] used sonochemical for the degradation of OFC. In this process, they used ultrapure water, Hydrogen peroxide, Argon gas, nitrogen, Oxygen, and an ultrasound generator. Here operating conditions play a major role in the degradation of OFC, like gas sparging, proper maintaining ultrasound power, and extra oxidants also present.

A. Thakur et al.[25] worked on the removal of OFC and paracetamol from an aqueous solution. In this experiment, they used rice husk as an adsorbent. The highest capacity of adsorbent is 7.54mg/g at pH 8, contact time 180 min, and adsorbent doses 100mg/10ml. They prepared AC from rice husk, and the functional group, a presence on the AC surface, is detected by “Fourier Transform Infrared Spectroscopy” (FTIR) analysis. The maximum value of “The Brunauer – Emmet Teller (BET) surface area is 127.48 m^2/g and the total pore volume is 0.3696.

V Bhatia, et al.[26] worked on OFC degradation from an aqueous solution using a Co-doped TiO_2 photocatalytic technique. The efficiency of this technique OFC degraded by about 86 %, at pH 3 after 6h, and the catalyst used 1.5g/l for 25ppm of OFC concentration. In this process, the most effective parameter is a catalyst, different sources of light, and doping ratio. The process is very difficult and complicated. In this process, chemicals are used like TiO_2 , $\text{Bi}(\text{NO}_3)_3 \cdot 5\text{H}_2\text{O}$, $\text{Ni}(\text{NO}_3)_2 \cdot 6\text{H}_2\text{O}$, etc. which are also expensive.

P. Papaphilippou et al.[27] produced nano-composite membrane via free radical polymerization polymer PMMA-co-PDEAEMA and magnetization using Iron oxide nanoparticles and uses as an adsorbent for OFC removal. The maximum removal rate occurs at 80 % at pH 4 at an adsorption time of 24h. In this process, the contact time is too high. They used magnetic nanocomposite using polymer. Also, they used several solvents like Tetrahydrofuran Ethyl acetate, ethanol, N-hexane, Chloroform, etc. which are more expensive and preparation of adsorbent is also a complex mechanism.

Q. Kong et al.[28] synthesized AC from luffa sponge activated with Phosphoric acid in a high ratio (1:5). g:ml, contact time 240 min. The AC goes through a two-step activation process namely physical and chemical processes. The resulting AC is used for the removal of

Ofloxacin. The adsorption process is suitable for the “pseudo-second order “ kinetic model and the Freundlich isotherm model

According to the research work of R. Wuana, et al.[29],AC obtained from Moringa Olifera pod for studying the removal of Ofloxacin. The samples were activated with saturated Ammonium Chloride solution, then carbonized at 623K. The Functional group determined of the prepared AC was by Fourier Transform Infrared Spectroscopy “FTIR” analysis. The BET surface area of AC is 235.79 m²/g and the maximum capacity is 5.051 mg/g.at 25°C,The resulting adsorption isotherm match with the Langmuir isotherm model. This absorption process is exothermic in nature.

G. Kaur et al.[30] developed AC from rice husk for the removal of OFC From aqueous solution. BET surface area of the samples is 32.6 m²/g and the adsorption capacity of this sample is 6.28 mg/g respectively.The prepared activated carbon showing maximum removal efficiency for Ofloxacin is 79.71% at neutral medium and the adsorption time is 430 min. The adsorption process is endothermic. Characterization of AC using X-ray diffraction (XRD).The adsorption capacity of the samples utilized a new technique, Central composite design which is based on the response Surface method.This process takes much more time than the removal of Ofloxacin.

M. Ashraf et al.[31] prepared activated carbon like granular activated carbon from coconut shells to investigate the removal ability of Danofloxacin and Ofloxacin from wastewater. The highest removal is 88% for Ofloxacin at an initial concentration of 30 ppm. The maximum removal rate was achieved at 240 min.The adsorption isotherm is fitted with the Temkin isotherm model.

P.King et al.[32] derived AC from Syzygium Cumini tree leaves for the removal of zinc. The prepared adsorbent has a maximum capacity of 35.84 mg/g followed by the Freundlich isotherm model. The adsorption process follows the pseudo-second-order kinetic model $R^2 = 0.99$.They experimented and prove that tree leaves have good adsorption capacity.

M.Vinayagam et al. [33] prepared activated carbon from Syzygiumcumini fruit shells. At first, the sample was carbonization done at 700°C and then activated by physical activation by passing CO₂. The time consumed for carbonization and activation is 6h. Prepared activated carbon characterized by “Fourier Transform Infrared Spectroscopy”(FTIR), “X-ray diffraction” (XRD), and “Scanning electron microscope” (SEM) analysis.

R. Araga et al. [34] synthesized AC from Jamun seed. The preparation of AC is two processes. At first, chemically activated by KOH at 2 days then the resulting sample was carbonized at 900°C. the time consumed by carbonization is 6hr 25 min. The adsorption capacity of the resulting sample is 3.65 mg/g. After the investigation effect of temperature, the kinetic of adsorption perfectly matched with the pseudo-second-order kinetic model. Gibbs's free energy at different temperatures is positive, which indicates the adsorption of Fluoride ions is non-spontaneous and exothermic in nature.

Vani et al.[35] developed activated Carbon from Jamun seed activated with Silver nitrate. From Jamun seed powder mixed, with Silver nitrate, they prepared silver nanoparticles. Using these samples they removed heavy metals from wastewater. The technique is very innovative but due to the high cost of silver nitrate the resulting nanoparticles are also costly. In the adsorption isotherm study, the equilibrium data was fitted with Langmuir and Freundlich adsorption isotherm.

A.Banerjee et al.[36] experimented on Jamun fruit about their antioxidant property. To determine various properties of Jamun seed they tested the Scavenging activity of the -OH group, Superoxide radical, lipid peroxidation, antioxidant capacity, etc. They proved that Jamun fruit has significant antioxidant activity.

F. Chavan et al.[37] prepared AC from Jamun leaves and uses it for the purification of domestic water. The prepared sample has a surface area of 250 m²/g. and having a carbon content of 65%. They proved that the AC sample eliminated a sufficient amount of COD present in the wastewater and jamun leaves have good adsorbent towards wastewater.

A. Jampani et al.[38] used jamun fruits for the purification of anthocyanins. The resulting AC had an adsorption capacity of 1.07mg/ ml and followed the second-order kinetic model. The desorption capacity of the adsorbent is 87%.

1.3 Purification technologies of removal of OFC from wastewater

1.3.1 Physical process

In this unit processes, screening, sedimentation floatation, and granular medium filtration occur. All of the process does not purify on a nano-scale. This process only purify at a certain value, and removed impurities from wastewater. But trace amounts of impurity are there, and this water can not be used for drinking purposes.

1.3.2 Biological process:

Activated sludge process, an aerated lagoon, and a Trickling filter are common examples of biological unit processes.

1.3.3 Activated sludge process

In this process, big amount of foam is produced, and some poisonous gas formed, like methane and sludge are produced high range of bacteria, viruses etc. which cause safety problems. Operating costs are the biggest disadvantage of this process.

1.3.4 Chemical processes :

The chemical processes can be classified by the following categories, which are discussed below.

❖ Photocatalytic Degradation :

In this process, solar sensitivity is used, in dark conditions. The process is also very costly. The major disadvantage of this process, it is very costly for operating purposes, and the instruments, which are used in this experiment also very expensive. Photocatalytic oxidation is not used for surface treatment. And the process is also complex.

❖ Membrane separation :

The process is used for domestic purposes, but for industrial scale, this process was not used due to maintaining cost, some hazardous solvents, Chemicals, destroy the membrane permanently. The rate of filtration is very slow larger species block the pore and the porosity of the membrane decreases.

❖ Coagulation :

In this process, investment is lower but the maintenance and operational cost is very high. In this process sometimes the formation of a large amount of residual non-biodegradable sludge creates a bad impact on the environment.

❖ Adsorption :

Nowadays adsorption process is largely used for domestic as well as industrial purposes. This technique has two phases, one is a solid phase, and another is a liquid or gaseous phase. One is adsorbent (solid phase) another is adsorbate. Adsorption is segregated as physical adsorption which causes by Van der Waals forces of attraction, water solubility, and particle size, and chemical adsorption occurs by sharing electrons, ion exchange, hydrogen bonding, etc.[39,40] Due to cost-effectiveness and low cost and

ease to use, the process is used largely. Adsorbents are in highly porous form and have a large surface area in the outer part, and diffusing molecules stay for a maximum time by magnetic forces towards the adjacent surface. In the batch study solution temperature is an important factor in the adsorption process, mostly in ambient temperature (25°C to 30°C) the maximum adsorption happened. The adsorption mechanism of pollutants depends on the solubility of pollutants. Water soluble compounds adsorb more rather than insoluble pollutants. The characteristics of an adsorbent are discussed below:

- The surface area should be a wide range
- Pores are equally distributed.
- The prepared adsorbent should have high capacity to remove the contaminant.
- Re-cycle and reuse-ability are also important factors.

This is a surface phenomenon and exothermic process, dependent on temperature.

1.4 Activated carbon as the adsorbent

Activated carbon (AC) is mainly two types: powder activated carbon, and granular activated carbon. One or both of these AC are manufactured through artificial ways followed by chemically activation or gas enactment of carbonous substances like coal, organic waste solid, wood, tires, luffa sponge willow peat, lignite, etc. can create the micro-crystalline kind of carbon known as activated carbon. For a lower adsorption framework cost, AC have recently been extracted from agricultural wastes such as, sugar cane, bagasse, coconut shell, rice husks, mango peel, and various tree leaves and barks, and fruits seed, etc. Preparation of activated carbon is carried out in a nitrogen atmosphere to remove air, for prevent yield loss and generation of nascent oxygen. temperature range increases from 450 to 700°C, in the pyrolysis process using the furnace. Due to their high porosity, larger surface area, dormant nature, security across a wide pH range, reasonable pore size, and presence of useful various organic functional groups, activated carbon is broadly utilized for natural micropollutants ejection from wastewater. The essential contrast between the granular activated carbon and powder activated carbon, that separates the two different types of adsorbents is that GAC has a more modest outer surface area and greater particles.

The adsorption technique assumes a significant part by surface area. During adsorption, the outer surface area impacts the pace of mass exchange, while the inside surface sets quite far as possible for the capacity of the adsorption process. The adsorption of normal particles onto the internal surface is also affected by the inward surface area of the material. Therefore, to facilitate the adsorption of significant particles, the pores should not be unreasonably little. There are various adsorbents available in the market among them activated carbon is the most common and useful. There are various adsorbents available in the market among them activated carbon is the most common and useful. From both phases either liquid (water) or gaseous, it widely removes organic contaminants. It also adsorbs low water-soluble compounds and removes them from water. This is used to remove non-degradable organic micro-pollutants and removal of pharmaceutical residue and also removes color from the solution. The preparation procedure of activated carbon is very simple and also prepare, from a natural resource, like tree leaves, hardwood, bark, fruit shell, etc.

In comparison with different trees, jamun seeds extract has some benefits such as a larger volume with an excellent affinity for binding, a wide surface area, and little need for nutrients. Jamun seeds (*Syzygium cumini*) are simple to grow in huge amounts in the environment, offering affordable feedstock for bio-adsorption. In recent times Jamun seed used as one of the resources of activated carbon due to its availability, low cost, and high physiochemical characteristics [32][36].

Jamun seeds were successfully used in this project work to prepare activated carbon using two steps, first pyrolysis using a muffle furnace, then chemically activated with potassium Hydroxide. Because Jamun seed is typical municipal waste and easily available, it was decided to use jamun seed as the main raw material of activated carbon. potassium hydroxide is used as a precursor because impregnated activated carbon conducted maximum removal of Ofloxacin from wastewater. To determine the optimal condition to perform the adsorption experiment, the factor affecting the process variable was carried out by adjusting process variable factors like adsorbent doses, contact time, and initial concentration, Kinetic studies are also carried out in addition to parameters studies. The purpose of the regeneration study was to determine whether the prepared adsorbent could be reused.

1.5 Objective of the work

Subsequently, after survey of previously mentioned literature, the expert discovered various water purification techniques including electrocoagulation[41] membrane filtration[42], advanced oxidation, Sonochemical degradation[12], fenton degradation[23] and many more. Although these techniques have their own benefit in water treatment purposes, it have several drawbacks also. The main disadvantage of sonochemical degradation, and membrane filtration, advanced oxidation techniques are high cost expensive. In Photocatalytic degradation process, handling of the Pyrex glass is too careful, the apparatus is very costly, and the mechanism is also complex. On the contrary adsorption technique for eliminating pollutants from wastewater is very convenient. The adsorption technique is an easy and inexpensive process.

Similarly, several adsorbents like neutral alumina, silica gel, zeolite, polymeric adsorbents, etc. are available for industrial purposes. But according to the above literature reviewed AC is the best option for wastewater treatment, because AC is less expensive than several adsorbents, and raw materials for preparing AC are from natural biomass sources. Pharmaceutical drugs like Ofloxacin are found in hospital wastewater. In appropriate intake of Ofloxacin can result in several kinds of disorders, like abdominal pain, chest pain, anxiety, fever, skin rash, and nervousness. So, Ofloxacin remediation from wastewater is therefore very crucial.

The thesis work concentrated mainly on OFC removal using activated carbon derived from jamun seed, and find its effectiveness in removing OFC from water. The activated jamun seed has enough potential, which enhances the removal effectiveness of OFC from its solution. The main goals of the research work are as follows.

- To make an adsorbent from biological resources, like waste jamun seed
- Development of activated carbon by carbonization using a muffle furnace at a certain temperature and thereafter, chemical activation by KOH at different ratio of carbonized jamun seed and KOH.
- Characterization of chemically activated jamun seed using SEM, BET, FTIR, particle size analyzer, CHNS and proximate analyser to determine the physical characteristics and composition of prepared activated carbon from jamun seed.

- The batch studies were carried out to find the effect of pH, initial ofloxacin concentration, amount of adsorbent dosage, temperature, and mixing time on the adsorption process.
- Testing of different isotherm such as Langmuir adsorption isotherm, Freundlich adsorption isotherm, Temkin adsorption isotherm using the jamun seed derived activated carbon.
- Study of kinetics of the adsorption process of OFC onto the surface of jamun seed derived activated carbon.
- Study of thermodynamic of the adsorption process of OFC onto the surface of jamun seed derived activated carbon.
- Regeneration studies of the prepared activated carbon from jamun seed.

CHAPTER 2

EXPERIMENTAL METHODOLOGY

2.1 Chemicals and biomass

Jamun (*Syzygium cumini*) fruit collected from the plantation situated at the Jadavpur University compound and also procured from vegetable market. Ofloxacin was purchased from Sigma-Aldrich. Potassium Hydroxide (KOH) was procured from Oasis Fine Chem, India. 25 % Ammonium Hydroxide (NH₄OH) and 37% Hydrochloric Acid (HCL) procured from Merck Specialities Pvt Ltd. Double distilled water was used throughout the experiment purposes preparing the aqueous solutions.

2.2 Preparation of activated carbon

The skin and outer part of jamun fruit were removed and the collected seeds were washed repeatedly with water to remove contaminants and impurities. Then, the seeds were sun-dried for seven days and subsequently dried in a hot air oven [Make: Spac-N-Service Hot Air Oven (Maximum temperature 300°C, 1.5 kW)] at 100°C for 48 h. After these procedures, the seeds were crushed and ground to a fine powder using mortar and pestle and sieved through a mesh size of 250 microns. Then the resultant powder is marked as jamun seed powder (JS) for the preparation of activated carbon. JS was then chemically activated in the following two-step processes. In the first step, the JS was carbonized in the programmable muffle furnace [Make: Spac-N-Service Muffle Furnace (Maximum temperature 1000°C, 4 kW)]. The carbonization process was carried out with a heating rate of 10°C/min from room temperature (~25°C) to the temperature of 350°C, thereafter, the temperature was held for 30 minutes to remove the organic matters, and finally, raising the temperature to 650°C with a heating rate of 10°C/min. Then, the process was maintained at 650°C for 2 hours for completion of carbonization process and lastly, it was left to cool down till room temperature was reached. The carbonized product was washed and decanted with distilled water several times to remove ash and dried in the oven at 120°C for 24 hours. The sample was labeled as carbonized jamun seed (CJS). In the second step, the CJS was chemically activated with KOH. It was treated with an aqueous solution of KOH taking different ratio of amount of KOH and CJS such as 1:1, 1:5, 1:10 and 2:1 by weight and was agitated at room temperature for 12 hours under magnetic stirring. Then, the solution was filtered and washed with water until the pH of the water became neutral. Finally, the chemically treated samples were dried in the hot-air oven at 120°C for 24 hours, ground, and stored in containers. This final product was named ACJS. The experimental process flow diagram is given in Figure 2.



Figure 2: Experimental steps to prepare ACJS from jamun seed (JS)

2.3 Characterization

The characterization of the jamun seed powder (JS) and subsequently prepared chemically activated jamun seed powder (ACJS) were performed by various analytical procedures to gather the knowledge of its surface morphology, functional groups, surface area and porosity measurement, chemical composition, and elemental composition prepared ACJS. They are elaborated in the following sections.

2.3.1 Ultimate analysis of JS

The total nitrogen, carbon, and sulfur of the JS and the prepared activated carbon (ACJS) were determined using an elemental analyzer (make:Elementar, model: vario cube). For the CHNS analysis, dried crushed samples were weighed (2-5 mg) in a tin capsule, which is then combusted in a reactor at a temperature of 1150°C. The tin capsule with sample melt and the tin promotes a violent reaction (flash combustion) in a temporarily enriched oxygen atmosphere. The combustion products CO₂, SO₂, and NO₂ were carried by a constant flow of carrier gas (helium) that passes through a glass column packed with an oxidation catalyst of tungsten trioxide (WO₃) and a copper reducer, both kept at 850°C. At this temperature, the nitrogen oxide was reduced to N₂. The N₂, CO₂, and SO₂ are then transported by the helium too, and separated by a 2 m long packed column and quantified with a thermal conductivity

detector set at 300°C). The CHNS elemental contents are reported in weight percent. The oxygen contents were calculated by difference.

2.3.2 Proximate analysis of JS

The amount of moisture in the JS sample was determined using the following procedure: 5 g of sample was added to vials, which was weighed beforehand. The vials were placed in an oven at 110°C, dried before being transferred into a desiccator for 1 hr, and reweighed to determine the percentage of moisture in the sample.

Ash content determination was done according to the ASTM D2866-94 method. Dry JS sample (1.0 g) was placed in a porcelain crucible and transferred into a preheated muffle furnace set at a temperature of 450°C. The furnace was left on for 30 minutes, after which the crucible and its content was transferred to another muffle furnace preheated at a temperature of 775±25°C. The crucible was left in the second muffle furnace for 1 hr. The crucible was then taken out and allowed to cool. The crucible and content were reweighed, and the weight loss was recorded as the ash content of the raw sample. Then the % ash content (dry basis) was calculated from Eq. (1).

$$\text{Total ash \%} = [(D1 - B1) \div (C1 - B1) \times 100] \quad (1)$$

where,

B1 = Weight of crucible (g)

C1 = Weight of crucible with original sample (g)

D1 = Weight of crucible with ashed sample (g)

Volatile organic matter content (wt%) was determined by the ASTM 5832 method. Approximately 1 g of the JS sample was taken in a crucible with cover (of known weight). The covered crucible was placed in muffle furnace regulated at 4950 °C for 7 min. Then the covered crucible was cooled to room temperature in a desiccator and recorded for the weight. The percentage weight loss was regarded as the percentage of volatile matter.

$$\text{Volatile organic content \%} = (D1 - B1) \div (C1 - B1) \times 100, \quad (2)$$

where,

B1 = Weight of crucible (g)

C1 = Weight of crucible with original sample (g)

D1 = Weight of crucible with burnt sample (g)

Fixed carbon is a calculated value and it is the resultant of summation of percentage moisture, ash, and volatile matter subtracted from 100.

$$\text{Fixed carbon\%} = [100 - (\text{moisture\%} + \text{ash\%} + \text{volatile matter\%})] \quad (3)$$

2.3.3 Scanning electron microscope (SEM) and EDS analysis

In order to study the surface characteristic of the jamun seed powder (JS) and prepared activated carbon (ACJS), scanning electron microscopy (Make: FEI; Model: INSPECT F50) was employed to visualize the morphology of the samples. The scan settings were fixed at an emission current of 100 mA and an accelerator voltage of 10 kV. EDS analysis was also carried out to micro-scale chemical composition on the surface of ACJS.

2.3.4 BET analysis

Brunauer–Emmett-Teller (BET) analyzer[make: Quantachro meautosorb model: iQ2 (100-240V, 50/60Hz)] was utilized to determine the surface area, pore volume, and pore diameter of samples. At first, the samples were degassed at 250°C for 3hrs under nitrogen atmosphere to remove unwanted impurities from the prepared activated carbon. An estimation of the volume of gas adsorbed throughout a broad range of pressure differences at a particular temperature (liquid N₂ at 77K) gives an adsorption isotherm. By contrast, desorption isotherms are determined by eliminating gas as pressure drops. Then the resultant sample was placed into a BET analyzer, and the gas chamber was filled with liquid nitrogen. The Pore size and surface are calculated by plotting the volume of adsorbed and relative pressure (P/P_o) values. The equation is given below:

$$\frac{1}{W[(P_o/P)-1]} = \frac{1}{W_m C} + \frac{C-1}{W_m C} \frac{P}{P_o} \quad (4)$$

where, W is the amount of gas adsorbed, P/P_o is the relative pressure, W_m is the weight of adsorbate, and C is the BET constant.

2.3.5 Fourier transform infrared (FTIR) spectroscopy

The presence of functional groups in the prepared samples was investigated by Fourier transform infrared (FTIR) spectroscopy[make: Shimadzu, model: QATR]. The occurrence of

functional groups in both JS and ACJS were studied in the range of wavelength of 4000cm^{-1} to 400cm^{-1} .

2.5. Particle size analyzer

Particle size of the prepared activated carbon was analyzed by Malvern Zetasizer. The particle size of ACJS are analyzed by Dynamic Light Scattering (DLS) method.

2.5. Batch adsorption studies

Adsorption studies were carried out in a round bottom flask in batch mode by using a 100 mL aqueous solution of Ofloxacin (OFC) as the absorbate. A mass of the prepared ACJS was added to the flask and kept in an isothermal stirring condition. The experiments were performed in a laboratory incubator shaker with a stirring speed of 180 rpm with a known concentration of OFC. An equal volume of the solution was withdrawn at a certain time interval. The withdrawn sample was filtered through Whatman filter paper and the filtered solution was analyzed in UV-Visible spectrophotometer (make: Perkin Elmer, Model: lambda 365) to estimate the amount of OFC removed by measuring the absorbance of the solution. For the purpose of determining the concentration of OFC solutions in UV-Visible spectrophotometer, a standard stock solution of 100 ppm of OFC was prepared. The subsequent OFC solutions were prepared by diluting the aqueous stock solution. The solutions of 1.5, 3, 7.5, 12 and 15 ppm were prepared and the standard graph of concentration versus absorbance were plotted by measuring the maximum absorbance for OFC at 287 nm. The standard plot is shown in Figure 3. From the figure, the relation between absorbance and concentration was determined and it is given in Equation 5.

$$\text{concentration} = \frac{\text{absorbance}}{0.108} \quad (5)$$

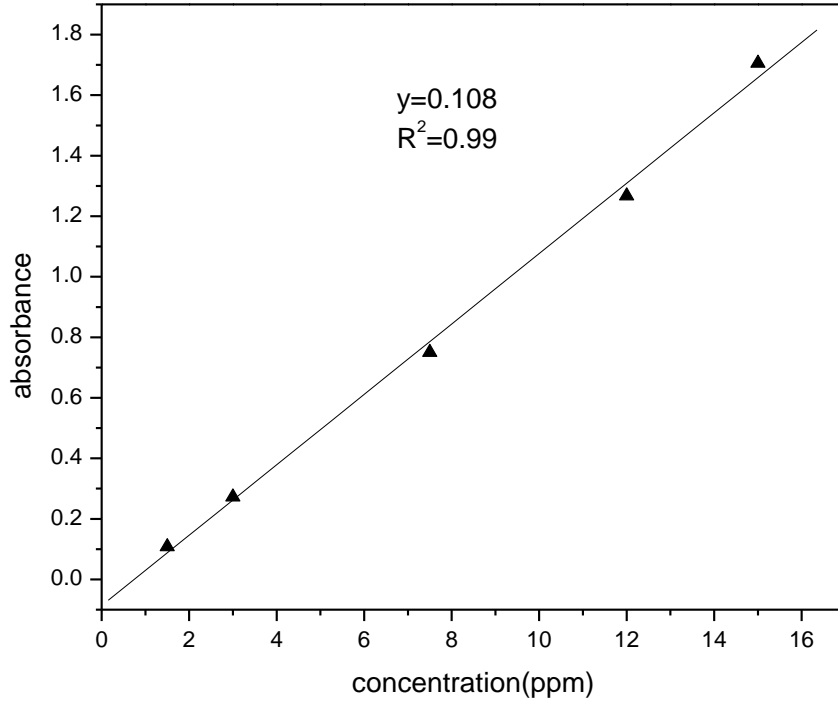


Figure 3: Standard plot to determine the concentration of OFC in aqueous solution

The removal percentages of OFC in batch adsorption studies were determined using the following formula

$$\text{Removal efficiency (\%)} = \frac{C_i - C_f}{C_i} \times 100 \quad (6)$$

where, C_i and C_f are the initial and final concentrations of OFC solution, respectively. The effect of ratio of KOH and CJS was studied to find out the best adsorbent in this study. The effect of various parameters such as solution pH, initial concentration, adsorbent dosage, and experimental time on the removal of OFC were measured. All the experiments were performed in triplicate.

The adsorption capacity (q_e), the amount of adsorbate adsorbed per unit weight of adsorbent at equilibrium, of the prepared ACJS for the removal of OFC, was calculated by the following equation.

$$q_e = \frac{(C_i - C_e)V}{m} \quad (7)$$

where, q_e is the adsorption capacity (mg/g), C_e is the final or equilibrium concentration of OFC (mg/L), C_i is the initial concentration of OFC (mg/L), V is the volume of aqueous solution (L), and m is the amount of adsorbent added (g).

2.5 Isotherm models to represent the adsorption process

When a solution comprising of adsorbate, comes in interaction with a solid adsorbent, molecules of adsorbate get transmitted from the solution phase to the compact solid phase until the concentration of adsorbate amongst the solution phase and the compact solid phase are in equilibrium. This is called adsorption equilibrium. Isotherms are the graphs showing distribution process of adsorption between the adsorbed phase and the solution phase at equilibrium. Various isotherm equivalences have been used to describe the equilibrium characteristics of adsorption.

2.5.1. Langmuir isotherm model

The Langmuir isotherm assumes that dynamic equilibrium occurs between adsorbed and free gaseous molecules. The adsorption involves the attachment of only one layer to the surface i.e. only monolayer adsorption is possible onto a surface with a finite number of similar active sites undergoing adsorption. Adsorption occurs at specific homogeneous active sites within the adsorbent. Adsorbent surface is uniform in terms of energy of adsorption. Adsorbed molecules do not interact with each other. Adsorbed molecules do not migrate on the adsorbent surface. The adsorption isotherm derived by Irving Langmuir for the adsorption of a solute from a liquid solution is given by Langmuir[43].

$$q_e = q_m \times \frac{K_L C_e}{1 + K_L C_e} \quad (8)$$

where, C_e is equilibrium or final concentration of dye (mg/L), q_e is amount of adsorbate adsorbed per unit weight of adsorbent at equilibrium (mg/g), q_m is amount of adsorbate adsorbed per unit weight of adsorbent required for monolayer adsorption i.e. maximum adsorption capacity of the adsorbent (mg/g) and K_L is amount of adsorbate adsorbed at equilibrium (L/mg). The linear form of Langmuir adsorption isotherm is

$$\frac{C_e}{q_e} = \frac{1}{q_m K_L} + \frac{C_e}{q_m} \quad (9)$$

The plot between C_e and C_e/q_e gives the calculation of Langmuir constants. Langmuir isotherm model can be utilized to evaluate the non-dimensional separation factor or the equilibrium parameter (R_L) by the following equation:

$$R_L = 1/(1 + K_L C_i) \quad (10)$$

where, is the equilibrium parameter and C_i is the maximum initial concentration. R_L values are indicative of the type of adsorption that is taking place, namely favorable ($0 < R_L < 1$), unfavorable ($R_L > 1$), linear ($R_L = 1$) or irreversible ($R_L = 0$).

2.5.2. Freundlich isotherm model

The Freundlich isotherm is an empirical relation between the solute concentrations on the adsorbent surface to the solute concentration in the contact liquid. It is obtained by considering heterogeneous surface with a non-uniform distribution of heat of adsorption. It assumes logarithmic decline in the heat of adsorption with increase in the extent of adsorption. It also indicates exponential variation in distribution sites with respect to adsorption energy. It does not show sufficient limit for monolayer filling. The non-linear form of adsorption isotherm derived by Freundlich shown below [44]:

$$q_e = K_F \cdot C_e^{1/n} \quad (11)$$

where, K_F is the adsorption coefficient that is indicative of the amount of adsorbate adsorbed on the surface of the adsorbent for a unit equilibrium concentration (L/mg) and n (dimensionless) is the Freundlich constant which determines the favorability of the adsorption process. The value of $1/n$ between 0 and 1 provides a quantitative measure of the adsorption intensity. A non-uniform distribution is pronounced when the value of $1/n$ approaches zero. On the other hand, a value of less than 1 for $1/n$ suggests that a normal Langmuir isotherm can explain the adsorption process while a value greater than 1 is a characteristic of cooperative adsorption. Linear form of Freundlich adsorption isotherm is given below.

$$\ln q_e = \ln K_F + \frac{1}{n} \ln C_e \quad (12)$$

The constants K_F and $1/n$ can be calculated by plotting the graph between $\ln C_e$ and $\ln q_e$.

2.5.3 Temkin adsorption isotherm model

Temkin isotherm model takes into account the effects of indirect adsorbate/adsorbate interactions on the adsorption process; it is also assumed that the adsorption heat of all molecules decreases linearly with the increase in coverage of the adsorbent surface, and that

adsorption is characterized by a uniform distribution of binding energies, up to a maximum binding energy. The Temkin isotherm can be described by Equation (13)[45].

$$q_e = \frac{RT}{b} \ln K_T + \frac{RT}{b} \ln C_e \quad (13)$$

where, K_T is Temkin isotherm constant (L/g) and b is the Temkin constant which is related to binding energy (J/mol). The plot between q_e and $\ln C_e$ gives the calculation of constants of Temkin isotherm.

2.6 Adsorption kinetic studies

Adsorption is the process by which solute molecules attach to the surface of an adsorbent. The adsorption process is done in batch or column setup. Kinetics of adsorption describes the rate of retention or release of a solute from an aqueous solution to solid interface at a given adsorbent dosage, temperature, flow rate and solution pH. During adsorption two main routes are involved; physical adsorption (physisorption) or chemical adsorption (chemisorption). Physical adsorption is as a result of weak van der Waals forces of attraction, whereas chemisorption involves the formation of a strong bond between the solute and the adsorbent that involves the transfer of electrons. Adsorption kinetics is one of the main factors that must be understood before the applicability of any adsorbent. In every adsorption process, linear or non-linear analysis of the kinetics is applied. Pseudo-First-order (PFO), Pseudo-Second-order (PSO), and Intra-particle (IP) model are some of the kinetics that forecasts the adsorbent-adsorbate interaction. The first two models have been widely applied in almost every sorption process. The suitability of any model depends on the error level—correlation coefficient (R^2) or Sum of Squared Errors (SSE). The linear forms have been applied to study the adsorption kinetics under batch adsorption experiments.

2.6.1 Pseudo first order kinetics

The pseudo first order kinetics is mostly used to analyze adsorption data obtained from the adsorption of adsorbates from aqueous solutions. It describes the rate of adsorption which is proportional to number of unoccupied binding sites on adsorbents and represented by the following mechanism;

$$\frac{dq_t}{dt} = k_1(q_e - q_t) \quad (14)$$

where, q_t is the adsorbate adsorbed onto adsorbent at time t (mg/g), q_e is the equilibrium adsorption capacity (mg/g), and k_1 is the pseudo first order rate constant per min. The integral

of Eq. (14) from $t=0$ to $t=t$ and $q_i=0$ and $q_t=q_t$ yields a linear expression of pseudo first order, Eq. (15).

$$\ln(q_e - q_t) = \ln q_e - k_1 t \quad (15)$$

The value of k_1 is determined by plotting $\ln(q_e - q_t)$ vs. t .

2.6.2. Pseudo second order kinetics

The pseudo second order kinetics describes the adsorption of adsorbates onto adsorbents where the strong chemical bonding between adsorbates and functional groups on the surface of adsorbents are responsible for the adsorption and the rate of adsorption of solute is proportional to the available sites on the adsorbent. Here the reaction rate is dependent on the amount of solute on the surface of the adsorbent—the driving force, $(q_e - q_t)$, is proportional to the number of active sites available on the adsorbent. The mechanism is given below:

$$\frac{dq_t}{dt} = k_2(q_e - q_t)^2 \quad (16)$$

where, k_2 is the pseudo second order rate constant (g/mg·min). The integral of Eq. (16) from $t=0$ to $t=t$ and $q_i=0$ and $q_t=q_t$ yields a linear expression of pseudo second order, Eq. (17).

$$\frac{t}{q_t} = \frac{1}{k_2 q_e^2} + \frac{t}{q_e} \quad (17)$$

A plot of t/q_t against t should demonstrate a linear system, from which the amount of adsorbate adsorbed at equilibrium (q_e , mg/g) and the equilibrium rate constant of pseudo-second-order sorption (k_2 , g/mg·min) can be evaluated from the slope and intercept, respectively. The pseudosecondorder kinetic model has been applied successfully to determine chemisorption in several sorption systems.

2.7 Intra-particle diffusion model

Intra-particle diffusion model has been widely applied to examine the rate limiting step during adsorption. The adsorption of solute in a solution involves mass transfer of adsorbate (film diffusion), surface diffusion, and pore diffusion. Film diffusion is an independent step, whereas surface and pore diffusion may occur simultaneously. Intra-particle diffusion was studied by Weber and Morris[46] and the linearized form of this model is given as

$$q_t = k_{ip} t^{\frac{1}{2}} + C \quad (18)$$

where, k_{ip} is the intra-particle diffusion constant ($\text{mg/g.min}^{0.5}$) and C is the boundary layer thickness. The values of C determines the boundary layer effect higher values, the greater the effect. The plot of q_t vs $t^{\frac{1}{2}}$, gives a linear function. If the line passes through the origin, intra-particle diffusion controls the adsorption process. However, on many occasions, the plot does not pass through the origin and it gives multiple linear sections; these sections corresponds to different mechanisms that control the adsorption process. There are four main mechanisms that describe the transfer of solute from a solution to the adsorbent. The first is called mass transfer (bulk movement) of solute particles as soon as the adsorbent is dropped into the solution. This process is too fast, thus it is not considered during the design of kinetic systems. The second mechanism is called film diffusion; it involves the slow movement of solutes from the boundary layer to the adsorbent's surface. When the solute reach the surface of the adsorbent, they move to the pores of the adsorbent—third mechanism. The final mechanism involves rapid adsorptive attachment of the solute on the active sites of the pores; being a rapid process, it is not considered during engineering design of kinetics. If the system is characterised by poor mixing, small solute size, and low concentration, film diffusion becomes the rate controlling step; otherwise, intra-particle diffusion controls the process.

2.8 Adsorption thermodynamic studies

According to chemist Jacobus Van't Hoff chemical thermodynamics for a given chemical reaction determine the internal heat energy, enthalpy, and entropy and free energy values of the system during chemical or physical transformation and inspect how they are dependent onto the reaction conditions. Inspection of the thermal parameters that accompany chemical reactions and the thermal properties of the reactants like Gibbs free energy change (ΔG^0), change in entropy (ΔS^0) and enthalpy (ΔH^0) are major parameters which govern the feasibility and spontaneity could make it possible to lay forward a general measure about the spontaneity of the reaction and helps to obtain information about the equilibrium.

The Gibbs free energy change (ΔG^0) is related to the adsorption equilibrium constant by the standard Van't Hoff equation:

$$\Delta G^0 = -RT \ln K \quad (19)$$

According to thermochemistry, the Gibbs free energy change (ΔG^0) is also related to the change in entropy (ΔS^0) and heat of adsorption (ΔH^0) at fixed temperature. It is shown by the following equation:

$$\Delta G^0 = \Delta H^0 - T\Delta S^0 \quad (20)$$

Combining the above two equations, result in the following equation:

$$\ln K = \frac{-\Delta G^0}{RT} = \frac{\Delta S^0}{R} - \frac{\Delta H^0}{R} \frac{1}{T} \quad (21)$$

where, K is the single point or distribution coefficient and is the ratio of q_e to C_e , ΔG^0 is the free energy change in kJ/mol, ΔH^0 is the change in enthalpy in kJ/mol, ΔS^0 is the change in entropy in kJ/mol.K, T is the absolute temperature in K and R is the universal gas constant i.e. 8.314 J/mol.K. Thus, thermodynamic parameter, ΔS^0 and ΔH^0 can be determined by the intercept and slope of the linear Van't Hoff plot i.e. as $\ln K$ versus $(1/T)$, respectively. Batch adsorption study was carried out at various temperature to determine the thermodynamic parameters.

2.9 Regeneration study

The exhausted ACJS were regenerated with eluents such as dilute HCl and dilute NH_4OH . All the regeneration experiments were carried out at room temperature. The exhausted ACJS was treated with 0.1M HCL or 0.1 M NH_4OH , washed with distilled water till neutral pH was achieved, and then, dried in hot air oven at 110°C for 24hr. The desorption and reuse of ACJS with initial adsorbent dosage of 1g/L, initial OFC concentration of 15 ppm, with solution pH~5, were evaluated for five regeneration cycles.

CHAPTER 3

RESULTS AND DISCUSSION

3.1 Characterization

3.1.1 Proximate and elemental analysis

The proximate composition of jamun seed is 28.1 wt% moisture, 18.6 wt% ash, 20.4 wt% volatile matter, and 32.9 wt% fixed carbon, which makes it suitable precursor for obtaining activated carbon. The ultimate analysis performed in CHNS analyzer is shown in Table 3 for JS and ACJS.

Table.3 The CHNS analysis of JS,ACJS

(%)	C	H	N	S
JS	55.68	15.91	1.85	0
ACJS	61.37	2.480	1.36	0.009

3.1.2 SEM-EDS

Scanning electron microscopy (SEM) is one of the most versatile and widely used of the surface analytical techniques as it allows both the morphology and composition of various materials in modern science to be studied. The surface micrograph of jamun seed powder (JS) and activated jamun seed powder (ACJS) were analyzed by FESEM analyzer and it is shown in Figure 4. It can be seen from the figure that after activation, the surface characteristics have changed considerably. The surface morphology of the ACJS as adsorbent exhibited nonuniformity with numerous the uneven surface with occasional cracks, pits, channels, and ridges which may have contributed to the increased surface area required for the OFC to interact with the adsorbent. In addition, various micro and macro pores facilitate adsorption on the ACJS surface. Moreover, it was found that the surface pores were of varying sizes and they were held responsible for the efficient adsorption performance. The pores were large enough to allow the OFC molecules to penetrate and get adsorbed on the surface after interacting with the functionalities present at those sites. The energy dispersive spectroscopy (EDS) technique is mostly used for qualitative analysis of materials but is capable of providing semi-quantitative results as well. The EDS spectrum of prepared ACJS is shown in Figure 5. The EDS spectrum evidently denoted the occurrence of only C atom in jamun seed while just K and O atoms in the KOH sample. This result is attributed to the reaction between KOH and C, which is considered the main reaction. It is expected that large amount of carbon decomposed by

reaction with potassium hydroxide[47]. Therefore, the activated carbons obtained by KOH activation have higher potassium and oxygen contents. In addition, the EDS spectrum of ACJS displayed that the ACJS contains carbon, potassium and oxygen as main elements and KOH reacts with CJS to form mostly oxidative compound K_2O .

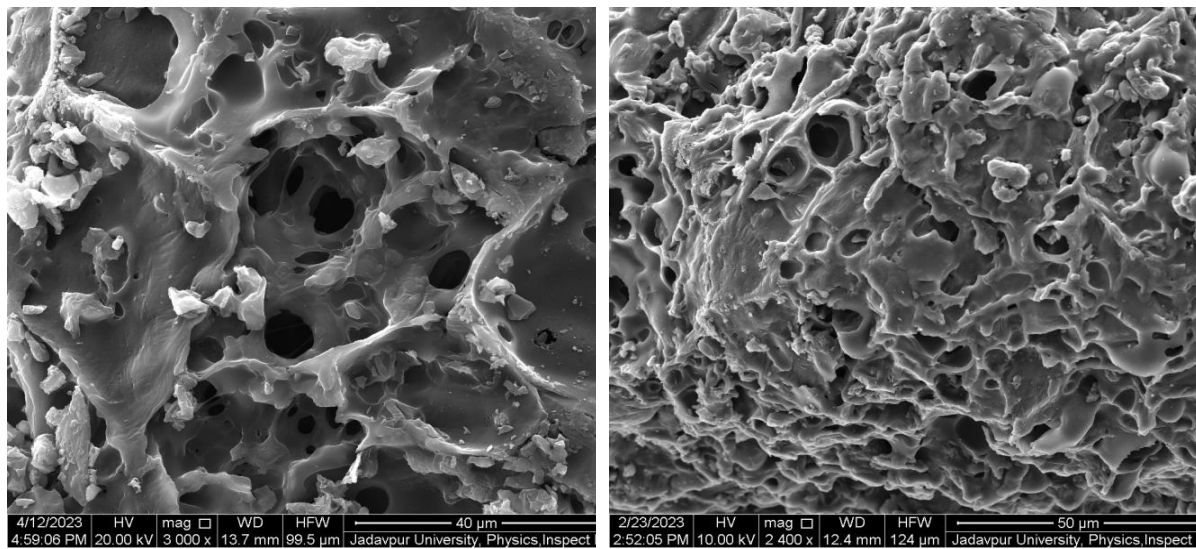


Figure 4: SEM morphology of (a) JS and (b) ACJS

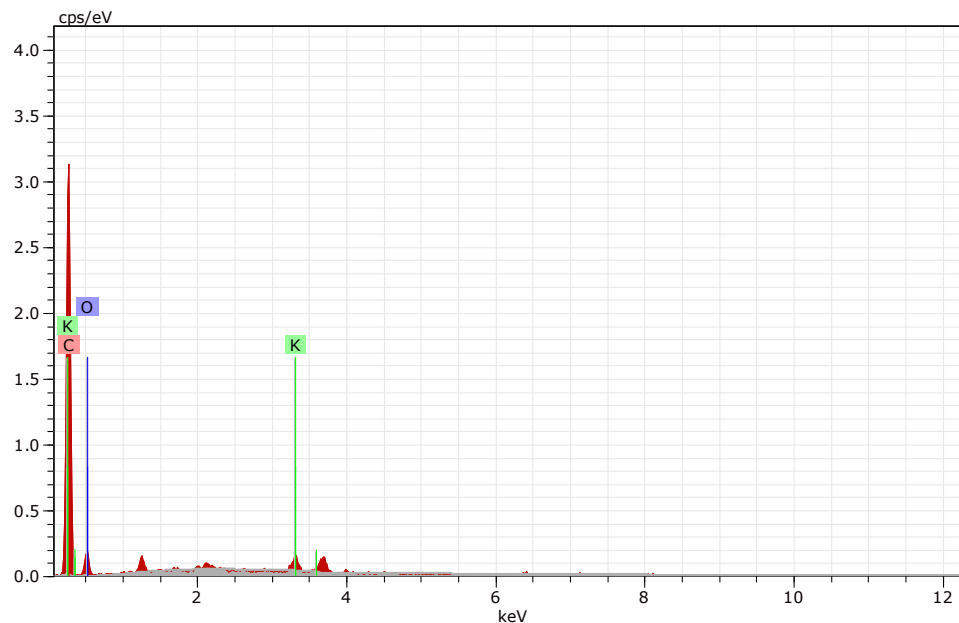
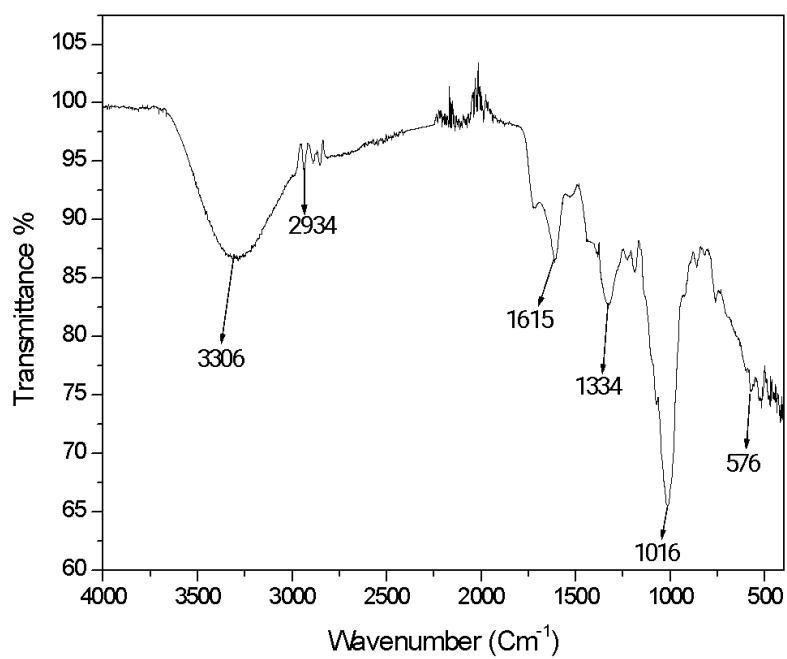


Figure 5: EDS spectrum of ACJS

3.1.3 FTIR analysis

Fourier-transform infrared spectroscopy (FTIR) analysis exhibits the infrared spectrum of absorption or emission of a material by collection of high-resolution spectral data over an extensive spectral range. It displays the extent of absorption of a single wavelength infrared light by a sample at each wavelength. The functional groups were identified in the FTIR spectrum between 400–4000 cm^{-1} and the result shown in Figure 6 for both JS and ACJS. The raw JS shows a broad band around 3306 cm^{-1} indicating O–H stretching (alcohol group). Also, this peak shows the presence of cellulosic components. The band at 2934 cm^{-1} confirms the presence of alkyl groups which is the indication of asymmetric C–H and alkyl groups (methyl and methylene group). The band 1615 cm^{-1} (C=C ring stretching) corresponds to aromatic compounds. Aliphatic ether C–O and alcohol (C–O stretching) components were confirmed by the peak of 1016 cm^{-1} . As shown in the figure, the activated sample possesses lower transmittance than the carbonized sample showing that ACJS has higher absorbance than the JS sample. After carbonization and subsequently KOH activation, all strong peaks like hexagonal, alkyl and alkanes groups disappeared, whereas aromatic groups are still visible. The shallow peaks were observed in the samples of ACJS at the band 1540 and 1001 cm^{-1} , which can be assigned to aromatic group (C=C ring stretching) and 2 adjacent H deformation, respectively. [48,49]

(a)



(b)

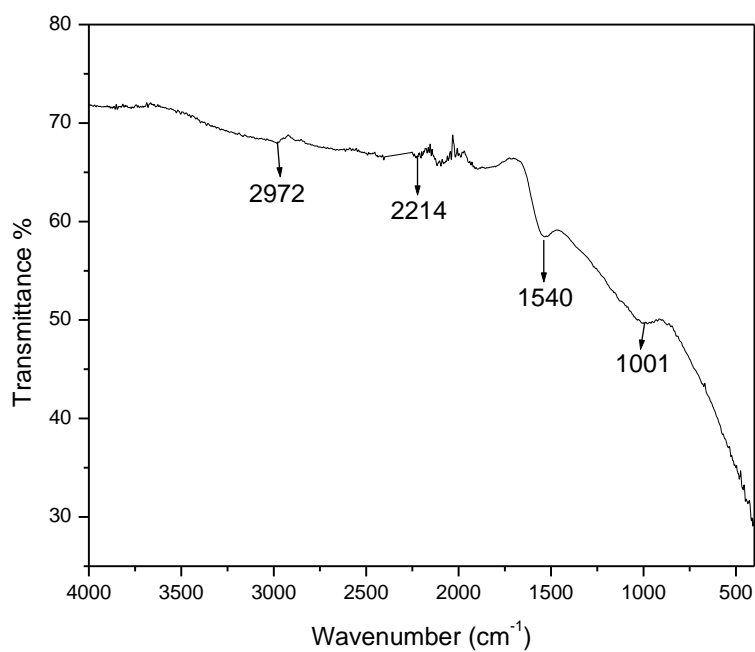


Figure 6: FTIR spectrum of (a) JS and (b) ACJS

3.1.4 BET analysis

The shape of N₂ adsorption–desorption isotherms can be different. The majority of physisorption isotherms may be grouped into the six types[50]. Type I isotherms are given by microporous solids having relatively small external surfaces (e.g.activated carbons, molecular sieve zeolites and certain porous oxides), the limiting uptake being governed by the accessible micropore volume rather than by the internal surface area. The reversible Type II isotherm is the normal form of isotherm obtained with a non-porous or macroporous adsorbent. The Type II isotherm represents unrestricted monolayer-multilayer adsorption. The reversible Type III isotherm is convex to the relative pressure axis over its entire range and therefore does not exhibit a Point B . Isotherms of this type are not common, but there are a number of systems. Characteristic features of the Type IV isotherm are its hysteresis loop, which is associated with capillary condensation taking place in mesopores, and the limiting uptake over a range of high relative pressure. The Type V isotherm is uncommon; it is related to the Type III isotherm in that the adsorbent-adsorbate interaction is weak, but is obtained with certain porous adsorbents. The Type VI isotherm, in which the sharpness of the steps depends on the system and the temperature, represents stepwise multilayer adsorption on a uniform non-porous surface. The step-height now represents the monolayer capacity for each adsorbed layer and, in the simplest case, remains nearly constant for two or three adsorbed layers.

The nitrogen adsorption–desorption isotherms of prepared ACJS is shown in Figure 7. The isotherm belong to type II of IUPAC classification[50]. A Type II isotherm is associated with macroporous structure adsorbent with unrestricted monolayer-multilayer adsorption related to monolayer coverage and macroporous structure. By comparing with hysteresis loops, in ACJS is analogous to type H3, which related to wedge shaped pores[51].From the BET analysis, the specific surface area of pyrolyzed jamun seed (CJS) and the pore volume of the same were found to be as 391.3568 m²/g and 0.2254 cc/g, respectively. On the other hand, the specific surface area of chemically activated jamun seed (ACJS) and the pore volume of the same were found to be as 366.39m²/g and 0.2169 cc/g, respectively. The surface area of ACJS is comparatively high and good relative pressure indicates high monolayer coverage for OFC.[51–53]

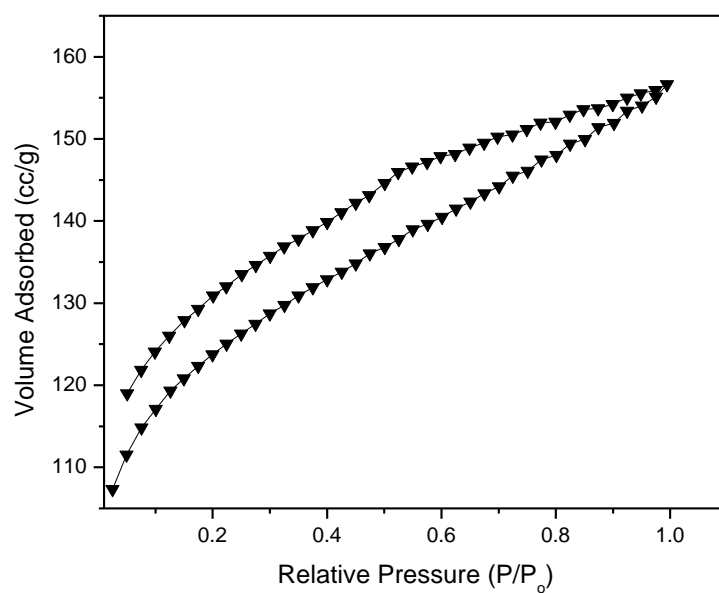


Figure 7:Hyteresis loop of ACJS in BET

3.1.5 Particle size analysis

The particle size distribution of ACJS is shown in Figure 8. The average particle size value was found to be as 602.38 nm.

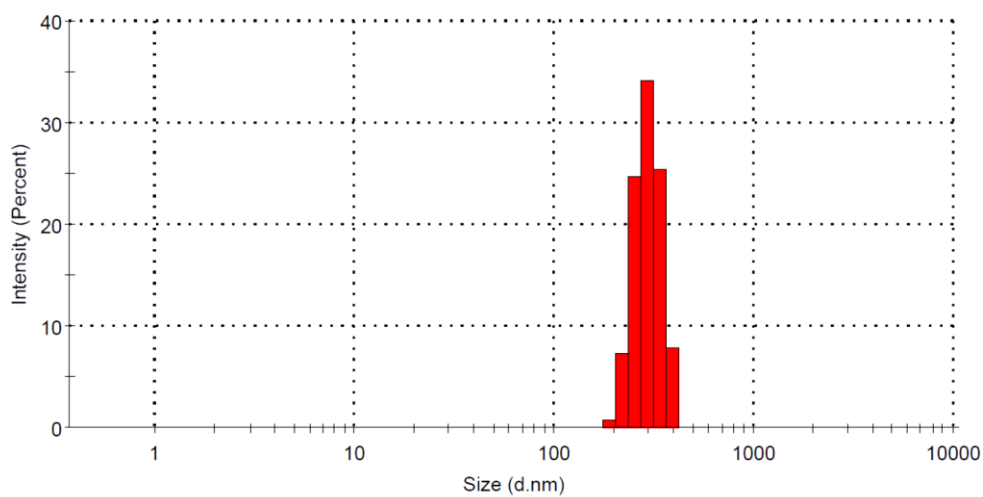


Figure 8: Particle size distribution of ACJS

3.2 Batch adsorption studies

3.2.1 Effect of ratio of KOH and CJS

The optimum adsorbent ACJS was chosen after developing various adsorbents obtained from activating via various ratios of KOH and CJS. The effect of ratio of KOH and CJS of the adsorbent on the removal performance of OFC at pH ~ 5 with temperature of 298K by taking the initial concentration of 15 ppm was carried out in the batch process and is shown in Figure 9. It is seen from the figure that the removal performance was increases with time of adsorption in all the cases. But, the maximum removal efficiency was found to be 96% after 210 minutes of contact time with the adsorbent that was chemically activated with KOH having the 1:1 ratio of KOH and CJS. So the adsorbent developed with 1:1 ratio KOH and CJS was taken as the optimum adsorbent in the present study and the further experiments were performed with the same adsorbent.

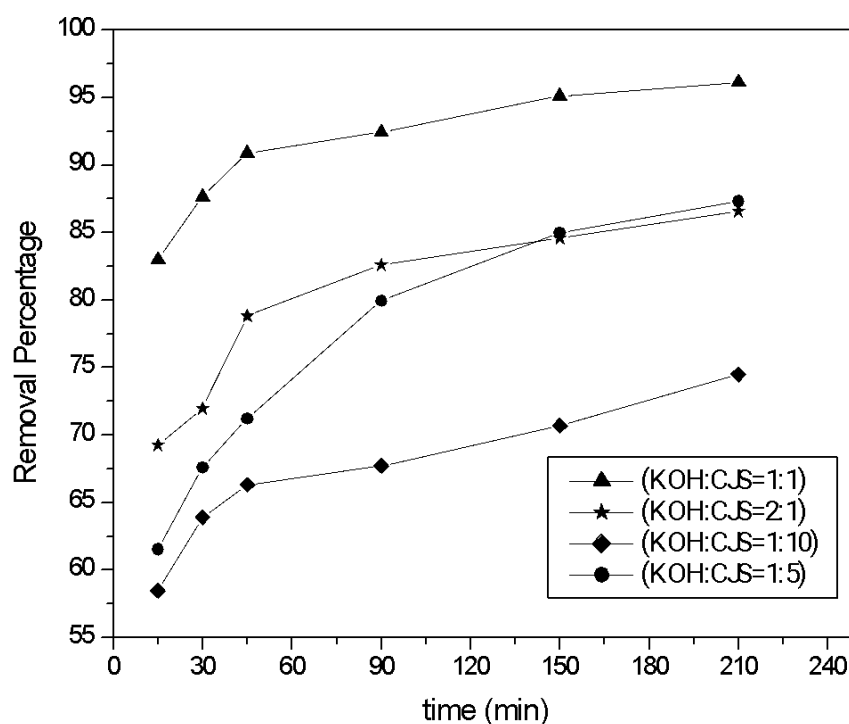


Figure 9: Effect ratio of KOH and CJS of adsorbents.

3.2.2 Effect of solution pH

The effect of pH on the OFC adsorption onto adsorbent, ACJS, was carried out at room temperature of 298K with the adsorbent dosage of 1g/L, initial OFC concentration of 15ppm,

for 210 minute and it is shown in Figure 10. It can be seen from figure that the adsorption is strongly dependent on pH. OFC removal increases with an increase in pH initially but, it decreases at higher pH before going through an optimum value. The highest percentage of Ofloxacin adsorption was recorded at pH 5. Ofloxacin is slightly acidic in nature. The Ofloxacin exists in different species at different ranges of pH. The pKa values of OFC are $pK_{a1}=5.45$ and $pK_{a2}=6.2$. [26] Ofloxacin is cationic below pK_{a1} (due to the presence of nitrogen in position 4 of the piperazinyl group), anionic above pK_{a2} (due to 6-carboxyl group), and zwitterionic i.e., neutral between pK_{a1} and pK_{a2} . [54] The adsorption will be governed by the pH of the solution, it can alter the adsorbent surface charge and chemical properties of the prepared ACJS and OFC solution [26,29]. As OFC contains negatively charged COO^- ion, at pH 5, slightly acidic medium has the highest removal rate of 96% due to the high ionic interaction between OFC and the charged surface of ACJS. It may be due to the fact that at a low pH value near 6, the H^+ ion concentration in the solution is attached to the OH^- ion of OFC in ACJS surface and as a result at pH ~5, the adsorption increases. [31,55]. At highly acidic conditions, at low pH ~3, the removal rate is 83 % due to the presence of the high H^+ ion concentration. At extremely low and high pH, cationic repulsion occurs and chemical change will also occur between OFC and surface of ACJS, which causes removal rate decreases. And at pH =5, a $\pi - \pi$ interaction occurs between $-OH$ group, and aromatic ring of OFC and ACJS, adsorption capacity of ACJS increases [28,56]. And it can be seen that aromatic ring of OFC and $\pi - \pi$ interaction should play a major role on the removal of OFC from aqueous solution. [57] A possible hydrogen bonding may also occur between ACJS surface and phenolic $-OH$ groups of OFC and increases adsorption on ACJS surface. [56] Also OFC has a fluorine group which has high electron withdrawing ability, and carboxyl group on aromatic ring has high π acceptor ability which also take part on adsorption. [58]. But at pH ~9 to pH ~10, at high value of pH, 20% of OFC has zwitterionic form and as a result decreases the adsorption of OFC on ACJS. [54] At very high pH or very low pH high electrostatic repulsion will occur between OFC and active surface of ACJS. [59] So, pH of the solution for adsorption process played a major important role for removal of OFC using ACJS from aqueous solution.

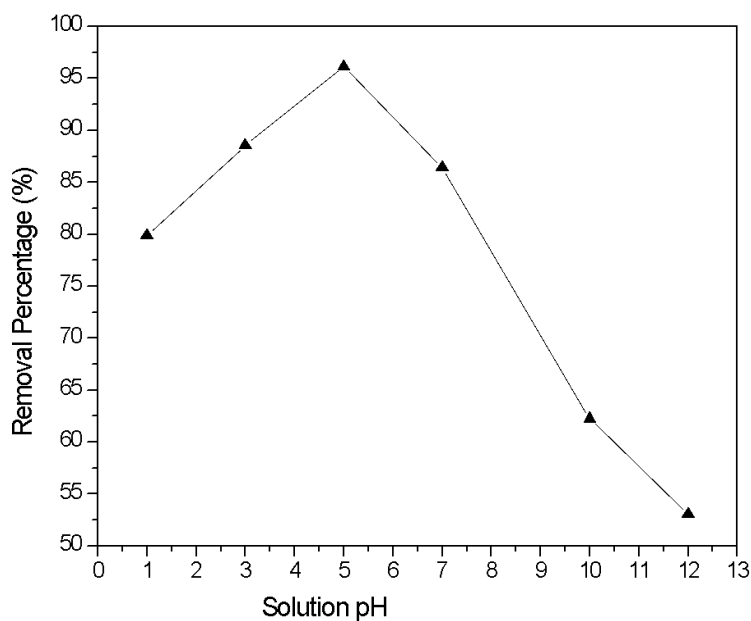


Figure 10: Effect of pH of solution

3.2.3 Effect of adsorbent dosage

The effect of ACJS dosages on removal of OFC at 15 ppm of initial OFC concentration with solution pH of 5 for 210 minutes adsorption time is shown in Figure 11. The amount of dosage was varied from 0.25 to 1.0 g/L of OFC solution under the optimized condition of agitation time. The result shows that by increasing the amount of adsorbent, the percentage removal also increases. At 0.25g/L ACJS dosage, the removal percentage of OFC was obtained as 40 % whereas, with the adsorbent dosage of 1.0 g/L, the removal percentage of OFC was found as 96 %. Various factors are reported which can cause the effect of adsorbent dosage. Those includes: (a) with an increase in the adsorbent dosage, the unsaturation of adsorption sites may lead to drop in adsorption capacity (b) agglomeration of adsorbent particles at higher doses may lead to reduce in the surface area and increase the diffusional path length[60,61].

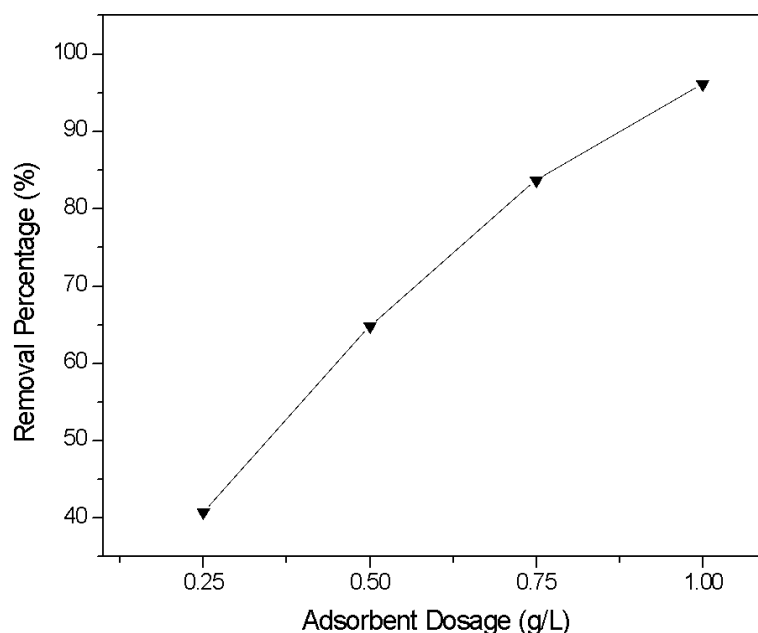


Figure 11: Effect of ACJS dosage on removal of OFC

3.2.4. Effect of initial concentration OFC

To study effect of initial concentration of OFC, prepared aqueous solution of OFC, at various concentration like, 15ppm, 24ppm, 30ppm, 45ppm, 60ppm, with pH=5, therefore adsorbent dosage 1g/L ACJS added on it. The incubator shaking speed 180 rpm, mixing time 210 minute. Effect of initial concentration is more important to calculate the capacity of prepared adsorbent, ACJS. Effect of initial concentration on the removal of OFC is shown in Figure 9. After nearly equilibrium reached, the percentage of removal for 15ppm OFC solution is 96.11 %, for 30ppm OFC solution the removal percentage 77 %, for 60ppm OFC solution the removal percentage is 68 %. With increasing initial concentration of OFC, the capacity of ACJS increases, but at the same removal efficiency decreases broadly, that was because the adsorbent surface area was fixed and active pore was insufficient for adsorbing large amount of OFC molecule in aqueous solution. The equilibrium adsorption capacity with the change in initial concentration of OFC is shown in Figure 12. It can be seen that in this study with increasing initial concentration equilibrium capacity raised 14.575 mg/g to 39.979 mg/g. Here with increasing concentration, no of active sites which act as driving force for adsorption [62] are filled, as a result removal efficiency decreases.

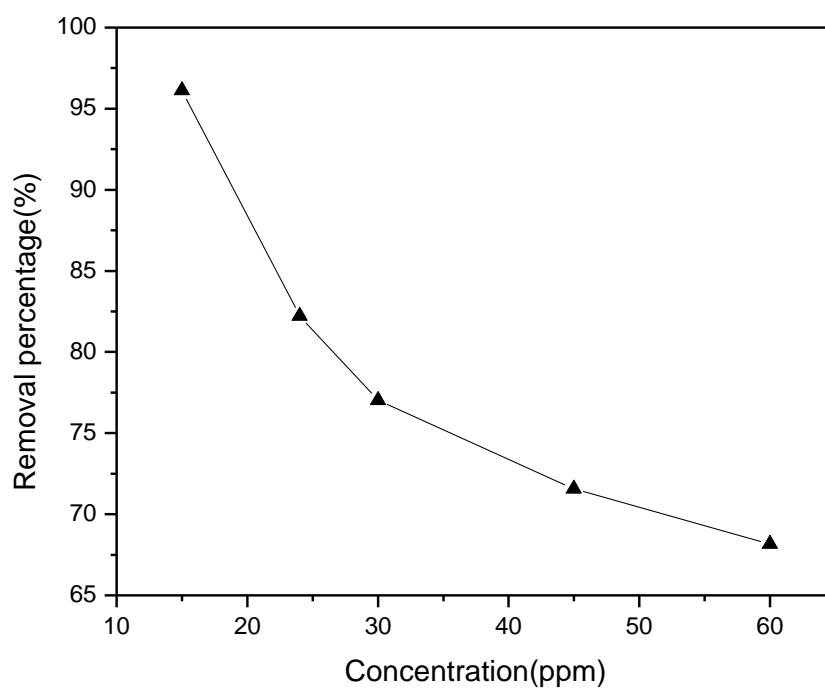


Figure 12.(a): Effect of initial concentration of OFC on removal efficiency of ACJS

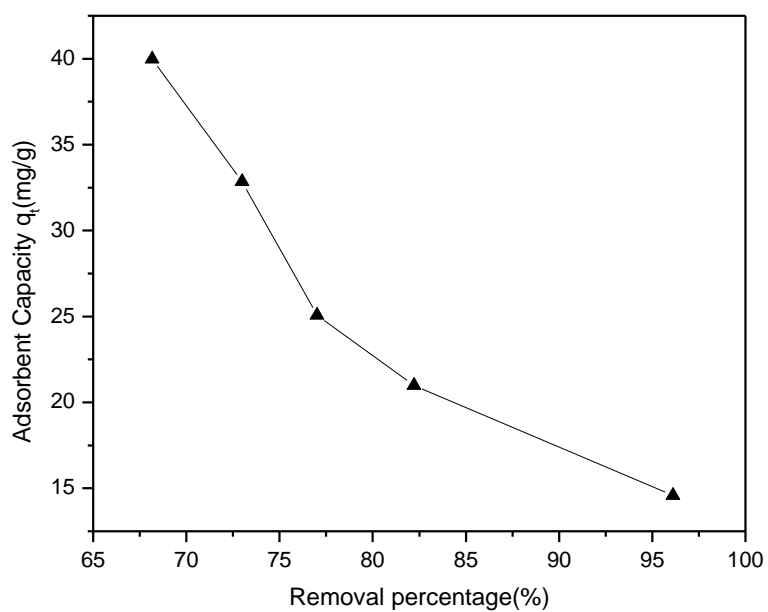


Figure 12.(b): Adsorbent capacity vs removal percentage of OFC.

3.2.5 Effect of temperature

After analyzing various parameters like pH, adsorbent dosage, mixing time, and initial OFC concentration, the effect of temperature was determined. To determine the impact of temperature on the adsorption of OFC, we studied 5 different temperatures, from 25°C to 50°C, at pH =5, adsorbent dosage 1g/l, initial OFC concentration 15ppm, and shaking speed is 180rpm. At 25°C the removal efficiency is 96%, and at 50°C the removal efficiency is 69%. From the experimental study, we see that as temperature increases from 25°C to 50°C the removal efficiency decreases from 96% to 69%, which shows that the adsorption of OFC is exothermic in nature.[55]. The removal of OFC is desirable at low temperature.

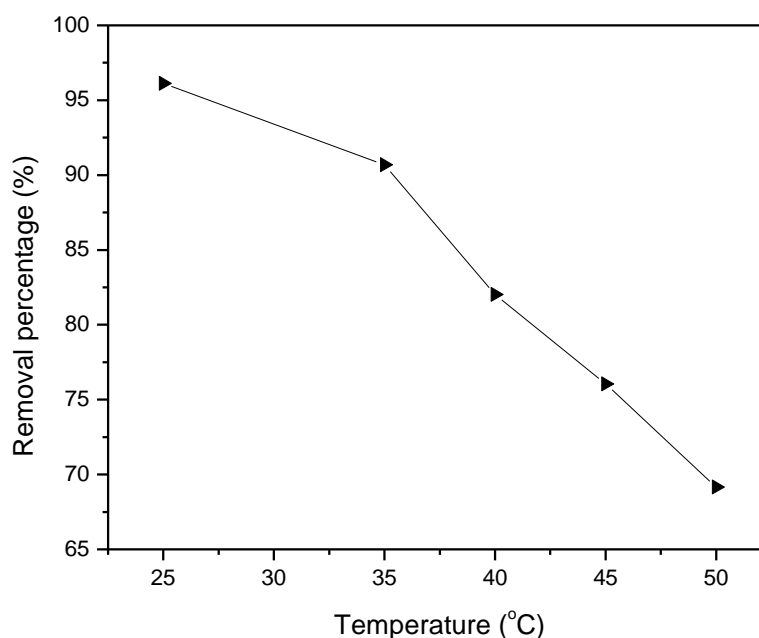


Figure 13:Effect of temperature on the removal of OFC

3.3. Isotherm studies

In the wastewater treatment process via adsorption technique to describe the whole work the adsorption isotherm is the most important parameter. The isotherm model predicts the linearity or non-linearity of the process. At certain temperatures, pH, and adsorbent dosage, by altering the concentration of OFC 15ppm to 60ppm, to evaluate the isotherm model. For designing an isotherm model equilibrium concentration is to be considered. Many researchers introduced

their model to predict adsorption isotherm. The various adsorption isotherm results carried out in this work are given in Table 5.

Table 4 . Experimental results on various adsorption isotherm

Adsorption Isotherm	Isotherm type	Equation	Plot	Results of Parameters
Langmuir Isotherm model	Non linear	$q_e = q_{max} \times \frac{K_L C_e}{1 + K_L \cdot C_e}$	q_e vs C_e	$q_{max}(\text{mg/g}) = 33.06$ $K_L (\text{Lmg}^{-1}) = 1$ $R^2 = 0.60$
	Linear	$\frac{C_e}{q_e} = \frac{1}{q_m K_L} + \frac{C_e}{q_m}$ $R_L = 1/(1 + K_L C_0)$	$\frac{C_e}{q_e}$ vs C_e	$q_m(\text{mg/g}) = 45.745$ $K_L (\text{Lmg}^{-1}) = 0.231$ $R^2 = 0.95$ $R_L = 2.24\text{E-}01$
Freundlich Isotherm model	Nonlinear	$q_e = K_F C_e^{1/n}$	q_e vs C_e	$K_F (\text{mg/g})(\text{mg/L})^n = 12.70$ $n (\text{g/L}) = 2.70$ $(1/n) = 0.36$ $R^2 = 0.92$
	Linear	$\log q_e = \log K_F + (1/n) \log C_e$	$\log q_e$ vs $\log C_e$	$K_F (\text{mg/g})(\text{mg/L})^n = 15.228$ $n (\text{g/L}) = 3.56$ $(1/n) = 0.28$ $R^2 = 0.9467$
Temkin Isotherm model	Linear	$q_e = \frac{RT}{b} \ln K_T + \frac{RT}{b} \ln C_e$	q_e vs $\ln C_e$	$K_T (\text{Lmg}^{-1}) = 5.914$ $b (\text{J/mol}) = 367.25$ $R^2 = 0.89$

After analyzing different adsorption isotherms, from the above table, the regression coefficient value is maximum for linear isotherm of Langmuir adsorption model; $R^2 = 0.95$, and maximum adsorption capacity $q_{\max}(\text{mg/g}) = 45.745$, but for the nonlinear model of Langmuir isotherm the regression coefficient $R^2 = 0.60$, maximum adsorption capacity is $33.06(\text{mg/g})$ so according to regression coefficient and adsorption capacity, comparing with different models of Langmuir adsorption isotherm, it was found that the adsorption capacity in linear model was greater than than the Langmuir non-linear model. Separation factor of Lanmuir isotherm was found as $R_L = 0.224$ (for linear isotherm). So for linear Langmuir adsorption isotherm, $R_L < 1$, the adsorption is favorable.[63] The linear and non-linear graphs are given in Figure 14(a) and Figure 14(b), respectively.

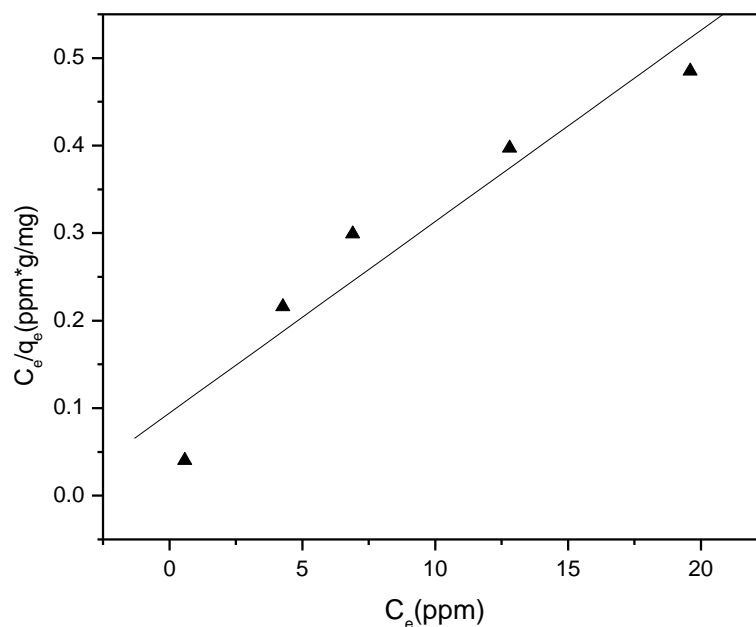


Figure 14 (a) Langmuir linear adsorption isotherm plot.

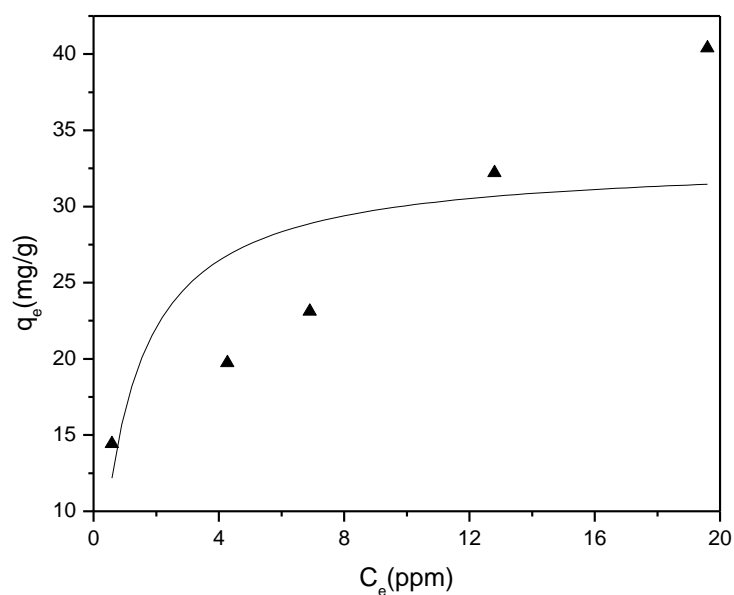


Figure 14(b) Nonlinear Langmuir Isotherm plot

After experimental study, it was to be seen that the regression coefficient of Freundlich linear model is 0.94, and for non linear model it is 0.92. Freundlich constant for linear isotherm is 15.22, and for non linear isotherm is 12.70. The calculated $(1/n)$ values for non linear isotherm 0.36, and that of for the linear isotherm is 0.28. The regression coefficient for linear Freundlich adsorption isotherm was greater than the that of the nonlinear Freundlich adsorption isotherm. The value of n was found as 3.56 for linear isotherm whereas, the value of n for non-linear isotherm was found as 2.7. The n values indicates the adsorption process is favourable.[64]The linear and non-linear plots of Freundlich adsorption isotherm are given in Figure 15(a) and Figure 15(b), respectively.

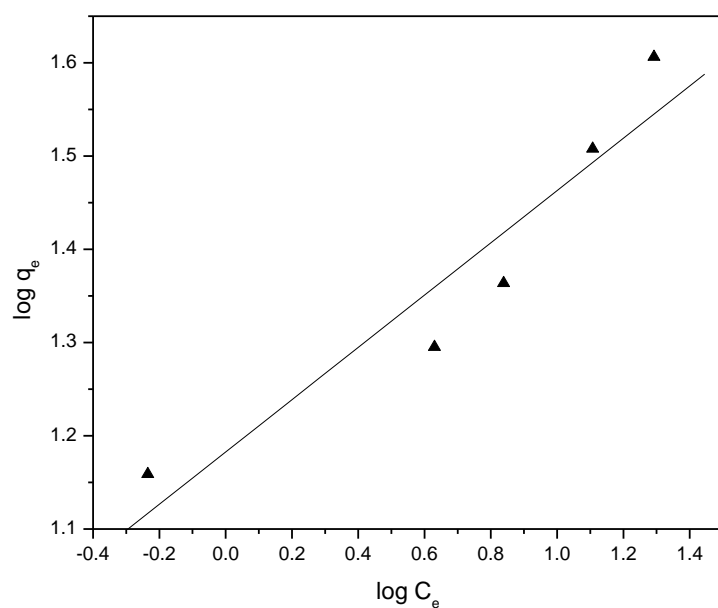


Figure 15 (a) Linear Freundlich adsorption isotherm model

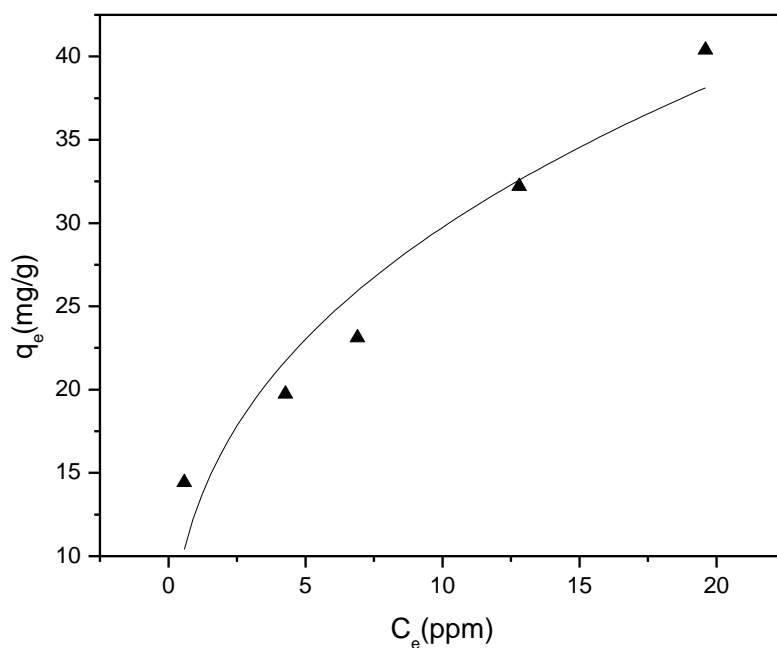


Figure 15(b) Non linear Freundlich adsorption isotherm model

Temkin adsorption isotherm is related to binding energy, and heat required during adsorption or heat of adsorption studies. Here we plot of equilibrium capacity vs logarithm of equilibrium concentration, q_e vs $\ln C_e$. From the intercept we get the value of Temkin constant K_T . In these studies the regression coefficient value of Temkin adsorption isotherm is 0.89, ($R^2 = 0.89$)

which shows that the adsorption of OFC does not suitable with Temkin adsorption isotherm. The Temkin constant $K_T = 9.56$ (l/mg). The plot of Temkin adsorption isotherm is given in Figure 16. So comparing the value of regression coefficient, it was found that Langmuir adsorption isotherm > Freundlich adsorption isotherm > Temkin adsorption isotherm.

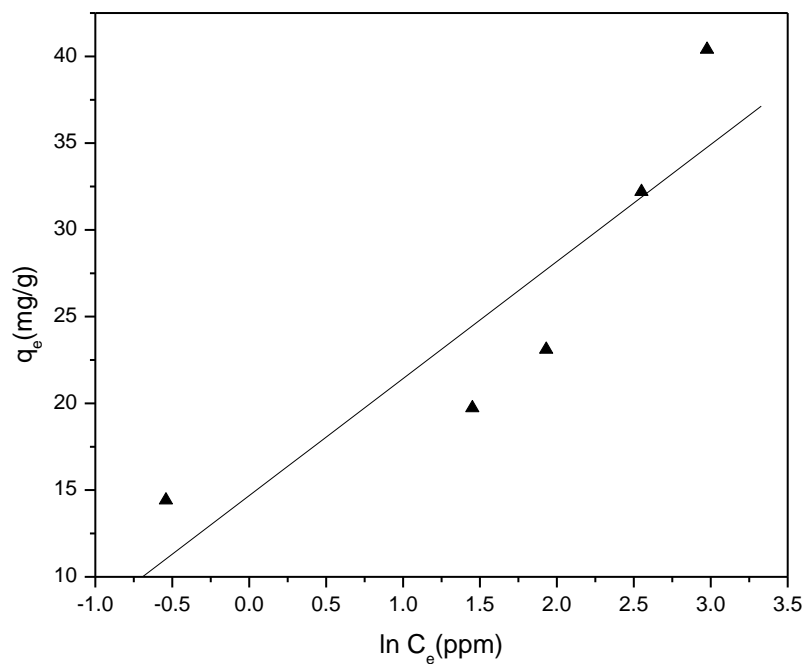


Figure 16 : Temkin adsorption isotherm

3.4. Kinetic Studies on Adsorption

Table 5. Results on adsorption kinetic model

Kinetic model	Type	Equation	Parameter	Experiment al capacity q _e (mg/g)
Pseudo 1 st order model	Linear	$\log(q_e - q_t) = \log q_e - \frac{K_1}{2.303} t$	q _{e,Cal} =2.537(mg/g) R ² = 0.98 K ₁ = 0.0179	14.4176
Pseudo 2 nd order model	Linear	$\frac{t}{q_t} = \frac{1}{K_s q_{eq}^2} + \frac{1}{q_{eq}} (t)$	q _e = 3.79(mg/g) K _s =1.01 R ² =0.99	
Intra-particle diffusion model	Linear	$q_t = K_i t^{\frac{1}{2}} + C$ q _t vs t ^(1/2)	R ² = 0.96 K _i = 0.17 C = 12.086	

The data of adsorption kinetics are given in the Table 6. In pseudo 1st order model, at first plot log(q_e-q_t) vs t. from the intercept and slope, we calculate the value of adsorption capacity and rate constant of pseudo 1st order model. From linear form of pseudo 1st order model, the calculated equilibrium capacity value q_{e,cal} = 2.537 mg/g are very less than the experimental capacity value. and rate constant of linear 1st order model K₁ = 0.0179, The graph of linear pseudo 1st order kinetics are given below.

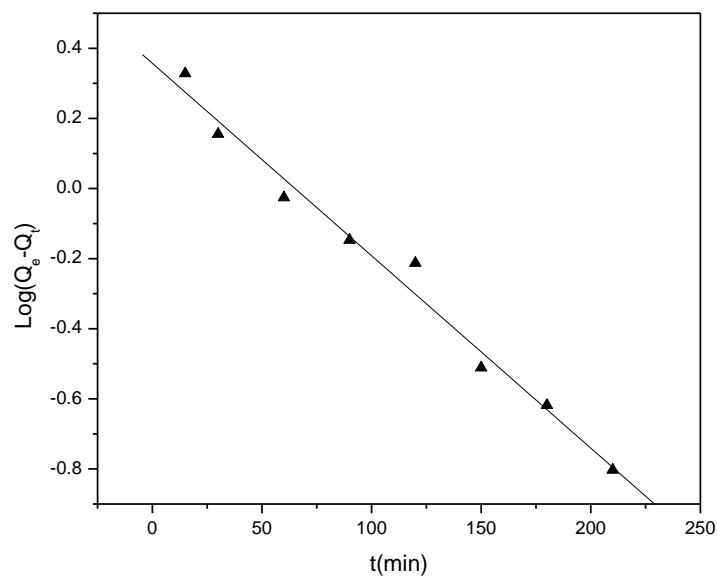


Figure 17(a) the plot of linear pseudo 1st order kinetics

After analyzed pseudo 1st order model we fitted the data with the pseudo 2nd order model. After plotting t/q_t vs t , for pseudo 2nd order linear model, we calculate capacity value (adsorbed OFC concentration) and 2nd order rate constant value from the slope, and intercept. From the table 6, it was to be seen that the adsorbed capacity $q_e = 3.79$ (mg/g) for linear pseudo 2nd order equation, and regression coefficient $R^2 = 0.99$. Also, it was found that 2nd order rate constant K_s linear kinetics is 1.01.

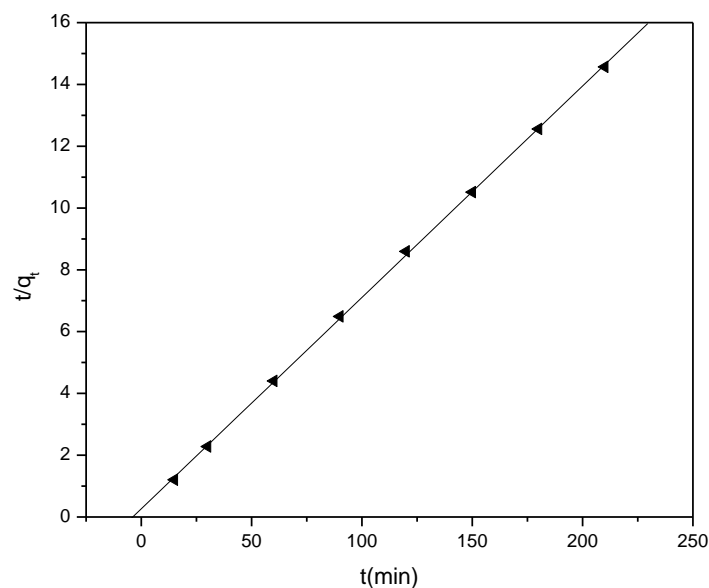


Figure 17(b) the plot of linear pseudo 2nd order kinetics.

In Intraparticle diffusion model after plotting q_t vs $t^{(1/2)}$, from slope we get the value of K_i intraparticle diffusion constant, and from intercept we get the C value. the regression coefficient of this diffusion model, $R^2 = 0.96$, and Intraparticle diffusion rate constant $K_i = 0.17$, C is model constant related to boundary layer = 12.086, standard deviation = 0.186. Here C value predicts about the thickness of boundary layer. From the study C value is higher, so adsorption of OFC has an effect of boundary layer. [65] From the Intraparticle diffusion model, it was stated that, from the plot of q_t vs $t^{(1/2)}$ if the straight line passes through the origin, then the adsorption model follows the Intraparticle diffusion model, but in this case the straight line does not pass through the origin, so the adsorption does not follow the Intraparticle diffusion model, but from the C value and regression coefficient R^2 value, the adsorption is influenced by the Intraparticle diffusion model.

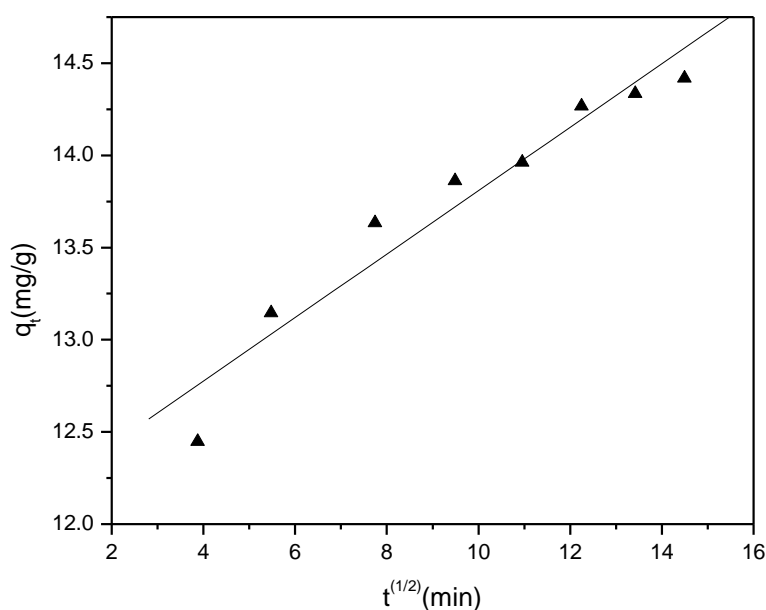


Figure 18 The plot of q_t vs $t^{(1/2)}$ for intraparticle diffusion model

3.5. Thermodynamics study on adsorption

Thermodynamic parameters are very important to check the spontaneity and feasibility of the adsorption process. They provide necessary information to design an adsorption process. Usually, thermodynamic parameters, that is, heat of enthalpy (ΔH), Gibbs free energy (ΔG), and entropy (ΔS). To describe the feasibility on adsorption of OFC by ACJS calculation of thermodynamic parameter are very important. The calculated value of thermodynamic parameter. Enthalpy, Entropy, Gibbs free energy are shown in the table 8. Using Vant'shoff equation, plot of $\ln K_d$ vs $(1/T)$ are shown in the figure 19. From the intercept of the plot $\ln K_d$ vs $(1/T)$, we calculate Entropy ΔS° and from the slope we calculate Enthalpy, ΔH° of this batch adsorption of OFC. Gibbs free energy ΔG° are calculated by using the equation $\Delta G^\circ = \Delta H^\circ - T\Delta S^\circ$, from different temperature 298K, 308K, 313K, 318K, and 323K The results are discuss below.

So from the below Table 8, it was to be seen that the entropy ΔS° negative, which indicates the disorderness between adsorbate and adsorbent molecules decreases during the adsorption of OFC[55]. It was to be seen that from the literature also the the entropy in adsorption of OFC, also negative and suggests randomness of adsorption decreases.[28,55]. During the adsorption

of OFC, the force of attraction between OFC molecules and ACJS molecules, and the OFC molecule get adhered to the surface of ACJS which cause decreases of Entropy of this batch adsorption process.[34].

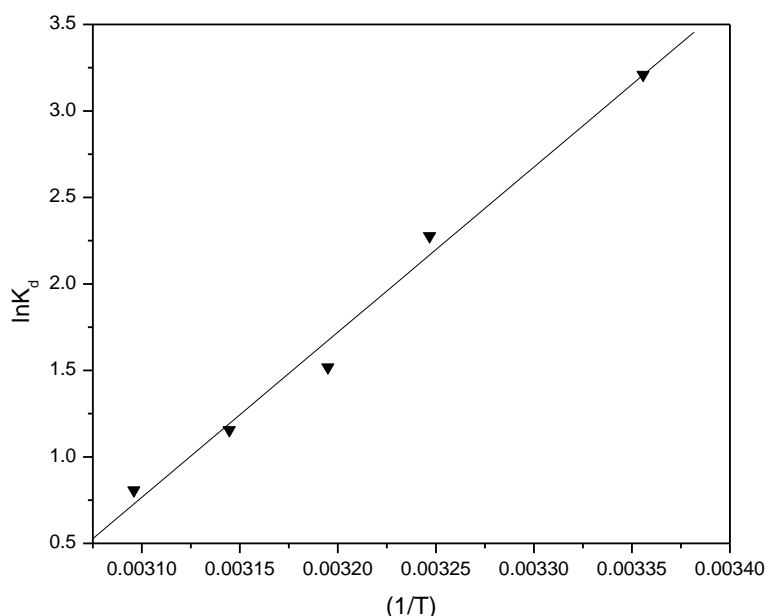


Figure 19 Thermodynamic study on adsorption of OFC,

The Gibb's free energy ΔG at 298K is -7.946 KJ/mol, at 308 K is -5.550 KJ/mol, at 323K is -1.95543 KJ/mol. The ΔG value at temperature 298K to 323K are negative which implies that the spontaneity and feasibility of the Adsorption of OFC.[31] The Enthalpy ΔH are negative. $\Delta H = -79.359$. means the adsorption is exothermic in nature, means with increasing temperature adsorption of OFC decreases. The activation energy calculated by plotting $\ln(1-\Theta)$ vs $(1/T)$ shown in the Figure 20. The calculated value of activation energy, $\Delta E = -68.7356$ KJ/mol.

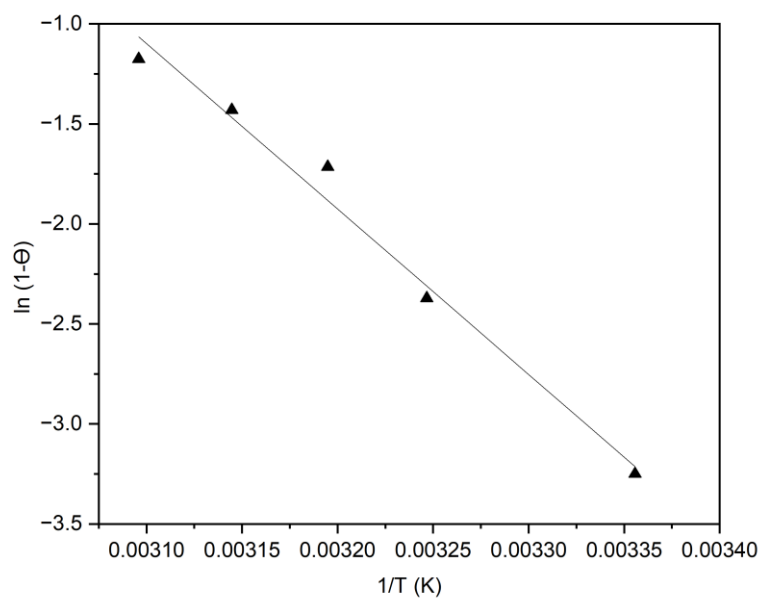


Figure 20. Determination of activation energy on adsorption.

Table 6 Represents the Thermodynamics studies

Thermodynamic Equation	Thermodynamic Parameter	Analytical value	
$S = (1 - \theta) \exp(-E_a/RT)$ $\theta = (1 - \frac{C_e}{C_0})$	E_a (KJ/mol)	-68.7356	
$\ln K_e = -\frac{\Delta H}{RT} + \frac{\Delta S}{R}$ plot of $\ln K_e$ vs $(1/T)$ $\Delta G^0 = \Delta H^0 - T\Delta S^0$	ΔH^0 (KJ/mol)	-79.3591	
	ΔS^0 (Jmol ⁻¹ K ⁻¹)	-239.64	
	ΔG^0 (KJ/mol) = $\Delta H^0 - T\Delta S^0$	T = 298 K	-7.94643
		T=308 K	-5.55003
		T=313K	-4.35183
		T=318K	-3.15363
		T= 323K	-1.95543

3.6. Regeneration study

In this batch adsorption study recycle of ACJS is most important for cost effective analysis. At first cycle initial adsorbent dose 1g/l, initial OFC concentration 15ppm, at pH=5, T= 298K, 180rpm , the removal efficiency 96 %. After 2nd and 3rd regeneration the removal efficiency drop down 89 % to 84 %. It was to be seen that the removal efficiency not so much lower.

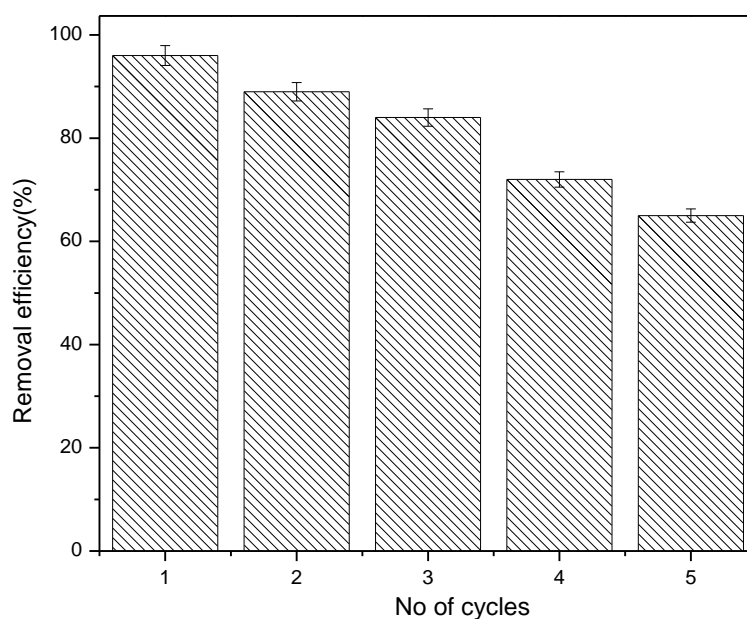


Figure 21 Regeneration studies of ACJS

But after 4th and 5th cycle the removal efficiency becomes 75% to 65%. After every cycle, adsorbent wash with 0.1M HCL solution, to remove unwanted particles. The batch adsorption of OFC is high at acidic medium, for purification of ACJS, acid treatment was done.

CHAPTER 4

4. Conclusion

In this project work the adsorbent (activated carbon) prepared from jamun seed for the removal of pharmaceutical drug , Ofloxacin. The ratio of KOH : pyrolysed jamun seed powder is (1:1) was best for the removal of OFC. A surface area of $366.39 \text{ m}^2/\text{g}$ was obtained for the activated carbon developed from jamun seed powder activated with KOH. The highest removal percentage of 96% of OFC by ACJS was found after 210 minutes of batch adsorption study. The adsorption isotherm was best fitted with linear Langmuir model, and the kinetics of the adsorption followed the pseudo 2nd order linear model. From the thermodynamics study the activation energy , entropy , entropy also negative, which indicates the adsorption is feasible and exothermic process($\Delta E = -68.7356 \text{ KJ/mol}$, $\Delta S = -239 \text{ J/mol.K}$, $\Delta H = -79.3591 \text{ KJ/mol}$). The maximum capacity of the ACJS for removal of OFC was obtained as 40.39 mg/g . So it can be concluded that the activated carbon derived from bio waste (jamun seed) was very useful for the removal of Ofloxacin from aqueous solution. The activated carbon which is derived from Jamun seed powder , also cost effective and can be utilized upto five cycles without compromising the removal efficiency of OFC from aqueous solution.

5. References

- [1] J. Akhtar, N.A.S. Amin, K. Shahzad, A review on removal of pharmaceuticals from water by adsorption, *Desalin. Water Treat.* 57 (2016) 12842–12860. <https://doi.org/10.1080/19443994.2015.1051121>.
- [2] A.J. Watkinson, E.J. Murby, D.W. Kolpin, S.D. Costanzo, The occurrence of antibiotics in an urban watershed: From wastewater to drinking water, *Sci. Total Environ.* 407 (2009) 2711–2723. <https://doi.org/10.1016/j.scitotenv.2008.11.059>.
- [3] P. Paíga, M. Correia, M.J. Fernandes, A. Silva, M. Carvalho, J. Vieira, S. Jorge, J.G. Silva, C. Freire, C. Delerue-Matos, Assessment of 83 pharmaceuticals in WWTP influent and effluent samples by UHPLC-MS/MS: Hourly variation, *Sci. Total Environ.* 648 (2019) 582–600. <https://doi.org/10.1016/j.scitotenv.2018.08.129>.
- [4] C.G. Daughton, T.A. Ternes, Pharmaceuticals and personal care products in the environment: Agents of subtle change?, *Environ. Health Perspect.* 107 (1999) 907–938. <https://doi.org/10.1289/ehp.99107s6907>.
- [5] M.D. Hernando, M. Mezcua, A.R. Fernández-Alba, D. Barceló, Environmental risk assessment of pharmaceutical residues in wastewater effluents, surface waters and sediments, *Talanta.* 69 (2006) 334–342. <https://doi.org/10.1016/j.talanta.2005.09.037>.
- [6] J.L. Martínez, Effect of antibiotics on bacterial populations : a multi-hierarchical selection process [version 1 ; referees : 2 approved] Referee Status :, 6 (2017) 1–10. <https://doi.org/10.12688/f1000research.9685.1>.
- [7] D.I. Andersson, D. Hughes, Antibiotic resistance and its cost: Is it possible to reverse resistance?, *Nat. Rev. Microbiol.* 8 (2010) 260–271. <https://doi.org/10.1038/nrmicro2319>.
- [8] D.I. Andersson, The biological cost of mutational antibiotic resistance : any practical conclusions ?, (n.d.). <https://doi.org/10.1016/j.mib.2006.07.002>.
- [9] S. Monarca, D. Feretti, C. Collivignarelli, L. Guzzella, I. Zerbini, G. Bertanza, R. Pedrazzani, The influence of different disinfectants on mutagenicity and toxicity of urban wastewater, *Water Res.* 34 (2000) 4261–4269. [https://doi.org/10.1016/S0043-1354\(00\)00192-5](https://doi.org/10.1016/S0043-1354(00)00192-5).
- [10] A. Gonsioroski, V.E. Mourikes, J.A. Flaws, Endocrine disruptors in water and their effects on the reproductive system, *Int. J. Mol. Sci.* 21 (2020). <https://doi.org/10.3390/ijms21061929>.
- [11] Z. He, S. Zang, Y. Liu, Y. He, H. Lei, A multi-walled carbon nanotubes-poly(l-lysine)

- modified enantioselective immunosensor for ofloxacin by using multi-enzyme-labeled gold nanoflower as signal enhancer, *Biosens. Bioelectron.* 73 (2015) 85–92.
<https://doi.org/10.1016/j.bios.2015.05.054>.
- [12] E. Hapeshi, A. Achilleos, A. Papaioannou, L. Valanidou, N.P. Xekoukoulotakis, D. Mantzavinos, D. Fatta-Kassinos, Sonochemical degradation of ofloxacin in aqueous solutions, *Water Sci. Technol.* 61 (2010) 3141–3146.
<https://doi.org/10.2166/wst.2010.921>.
- [13] J. Michael, *Formulary Forum, Ann. Pharmacother.* 23 (1989) 839–846.
- [14] K. Kümmerer, Antibiotics in the aquatic environment - A review - Part I, *Chemosphere.* 75 (2009) 417–434. <https://doi.org/10.1016/j.chemosphere.2008.11.086>.
- [15] Y. Deng, A. Debognies, Q. Zhang, Z. Zhang, Z. Zhou, J. Zhang, L. Sun, T. Lu, H. Qian, Effects of ofloxacin on the structure and function of freshwater microbial communities, *Aquat. Toxicol.* 244 (2022) 106084.
<https://doi.org/10.1016/j.aquatox.2022.106084>.
- [16] P. Kovalakova, L. Cizmas, T.J. McDonald, B. Marsalek, M. Feng, V.K. Sharma, Occurrence and toxicity of antibiotics in the aquatic environment: A review, *Chemosphere.* 251 (2020) 126351.
<https://doi.org/10.1016/j.chemosphere.2020.126351>.
- [17] M.S. de Ilurdoz, J.J. Sadhwani, J.V. Reboso, Antibiotic removal processes from water & wastewater for the protection of the aquatic environment - a review, *J. Water Process Eng.* 45 (2022) 102474. <https://doi.org/10.1016/j.jwpe.2021.102474>.
- [18] A. Al-ahmad, V. Mersch-sundermann, Biodegradability of some antibiotics , elimination of the genotoxicity and a € ction of wastewater bacteria in a simple test, 40 (2000).
- [19] M.A. Al-Omar, Chapter 6 Ofloxacin, 2008. [https://doi.org/10.1016/S1871-5125\(09\)34006-6](https://doi.org/10.1016/S1871-5125(09)34006-6).
- [20] A.Y.C. Lin, T.H. Yu, C.F. Lin, Pharmaceutical contamination in residential, industrial, and agricultural waste streams: Risk to aqueous environments in Taiwan, *Chemosphere.* 74 (2008) 131–141. <https://doi.org/10.1016/j.chemosphere.2008.08.027>.
- [21] D.G.J. Larsson, C. de Pedro, N. Paxeus, Effluent from drug manufactures contains extremely high levels of pharmaceuticals, *J. Hazard. Mater.* 148 (2007) 751–755.
<https://doi.org/10.1016/j.jhazmat.2007.07.008>.
- [22] S. Castiglioni, R. Bagnati, R. Fanelli, F. Pomati, D. Calamari, E. Zuccato, Removal of

- pharmaceuticals in sewage treatment plants in Italy, *Environ. Sci. Technol.* 40 (2006) 357–363. <https://doi.org/10.1021/es050991m>.
- [23] J. Liu, X. Wu, J. Liu, C. Zhang, Q. Hu, X. Hou, Ofloxacin degradation by Fe₃O₄-CeO₂/AC Fenton-like system: Optimization, kinetics, and degradation pathways, *Mol. Catal.* 465 (2019) 61–67. <https://doi.org/10.1016/j.mcat.2018.12.020>.
- [24] M.O. Composite, Fenton Degradation of Ofloxacin Using a, (2020) 2–11. <https://doi.org/10.3390/ECCS2020-07528>.
- [25] A. Thakur, N. Sharma, A. Mann, *Materials Today : Proceedings* Removal of ofloxacin hydrochloride and paracetamol from aqueous solutions : Binary mixtures and competitive adsorption, *Mater. Today Proc.* 28 (2020) 1514–1519. <https://doi.org/10.1016/j.matpr.2020.04.833>.
- [26] V. Bhatia, A.K. Ray, A. Dhir, Enhanced photocatalytic degradation of ofloxacin by co-doped titanium dioxide under solar irradiation, *Sep. Purif. Technol.* 161 (2016) 1–7. <https://doi.org/10.1016/j.seppur.2016.01.028>.
- [27] P.C. Papaphilippou, O.M. Marinica, E. Tanas, F. Mpekris, T. Stylianopoulos, V. Socoliuc, T. Krasia-christoforou, Ofloxacin Removal from Aqueous Media by Means of Magnetoactive Electrospun Fibrous Adsorbents, (2022).
- [28] Q. Kong, X. He, L. Shu, M. sheng Miao, Ofloxacin adsorption by activated carbon derived from luffa sponge: Kinetic, isotherm, and thermodynamic analyses, *Process Saf. Environ. Prot.* 112 (2017) 254–264. <https://doi.org/10.1016/j.psep.2017.05.011>.
- [29] R.A. Wuana, R. Sha’Ato, S. Iorhen, Aqueous phase removal of ofloxacin using adsorbents from Moringa oleifera pod husks, *Adv. Environ. Res.* 4 (2015) 49–68. <https://doi.org/10.12989/aer.2015.4.1.049>.
- [30] G. Kaur, N. Singh, A. Rajor, Ofloxacin adsorptive interaction with rice husk ash: Parametric and exhausted adsorbent disposability study, *J. Contam. Hydrol.* 236 (2021) 103737. <https://doi.org/10.1016/j.jconhyd.2020.103737>.
- [31] M. Ashraf, M.M. Galal, M.E. Matta, Removal of danofloxacin and ofloxacin as different generations of fluoroquinolones from aqueous solutions through the adsorption process using granular activated carbon: A comparative study, mechanism elucidation, and applicability investigation, *Alexandria Eng. J.* 71 (2023) 679–690. <https://doi.org/10.1016/j.aej.2023.03.096>.
- [32] P. King, N. Rakesh, S.B. Lahari, Y.P. Kumar, V.S.R.K. Prasad, Biosorption of zinc onto *Syzygium cumini* L.: Equilibrium and kinetic studies, *Chem. Eng. J.* 144 (2008)

- 181–187. <https://doi.org/10.1016/j.cej.2008.01.019>.
- [33] M. Vinayagam, R. Suresh Babu, A. Sivasamy, A.L. Ferreira de Barros, Biomass-derived porous activated carbon from *Syzygium cumini* fruit shells and *Chrysopogon zizanioides* roots for high-energy density symmetric supercapacitors, *Biomass and Bioenergy*. 143 (2020) 105838. <https://doi.org/10.1016/j.biombioe.2020.105838>.
- [34] R. Araga, S. Soni, C.S. Sharma, Fluoride adsorption from aqueous solution using activated carbon obtained from KOH-treated jamun (*Syzygium cumini*) seed, *J. Environ. Chem. Eng.* 5 (2017) 5608–5616. <https://doi.org/10.1016/j.jece.2017.10.023>.
- [35] REMOVAL OF HEAVY METAL FROM WASTE WATER BY ADSORPTION USING CHEM-BIO MODIFIED BIO DEGRADABLE WASTE WITH THE HELP OF SILVER NANO PARTICLES FROM, 6 (2018) 1298–1318.
- [36] A. Banerjee, N. Dasgupta, B. De, In vitro study of antioxidant activity of *Syzygium cumini* fruit, *Food Chem.* 90 (2005) 727–733. <https://doi.org/10.1016/j.foodchem.2004.04.033>.
- [37] F.I. Chavan, M. Husain, S.S. Paul, I. Mohammad, Domestic Wastewater Treatment Using Jamun Leaves As Adsorbents, *Int. J. Innov. Eng. Sci.* 6 (2021) 1. <https://doi.org/10.46335/ijies.2021.6.10.1>.
- [38] C. Jampani, A. Naik, K.S.M.S. Raghavarao, Purification of anthocyanins from jamun (*Syzygium cumini* L.) employing adsorption, *Sep. Purif. Technol.* 125 (2014) 170–178. <https://doi.org/10.1016/j.seppur.2014.01.047>.
- [39] E.S. Rigobello, A.D.B. Dantas, L. Di Bernardo, E.M. Vieira, Removal of diclofenac by conventional drinking water treatment processes and granular activated carbon filtration, *Chemosphere*. 92 (2013) 184–191. <https://doi.org/10.1016/j.chemosphere.2013.03.010>.
- [40] E. Arany, J. Láng, D. Somogyvári, O. Láng, T. Alapi, I. Ilisz, K. Gajda-Schranz, A. Dombi, L. Kohidai, K. Hernádi, Vacuum ultraviolet photolysis of diclofenac and the effects of its treated aqueous solutions on the proliferation and migratory responses of *Tetrahymena pyriformis*, *Sci. Total Environ.* 468–469 (2014) 996–1006. <https://doi.org/10.1016/j.scitotenv.2013.09.019>.
- [41] M. Negarestani, M. Motamedi, A. Kashtiaray, A. Khadir, M. Sillanpää, Simultaneous removal of acetaminophen and ibuprofen from underground water by an electrocoagulation unit: Operational parameters and kinetics, *Groundw. Sustain. Dev.* 11 (2020). <https://doi.org/10.1016/j.gsd.2020.100474>.

- [42] B. Maryam, V. Buscio, S.U. Odabasi, H. Buyukgungor, A study on behavior, interaction and rejection of Paracetamol, Diclofenac and Ibuprofen (PhACs) from wastewater by nanofiltration membranes, *Environ. Technol. Innov.* 18 (2020) 100641. <https://doi.org/10.1016/j.eti.2020.100641>.
- [43] I. Langmuir, THE ADSORPTION OF GASES ON PLANE SURFACES OF GLASS, MICA AND PLATINUM., *J. Am. Chem. Soc.* 40 (1918) 1361–1403. <https://doi.org/10.1021/ja02242a004>.
- [44] H.M.F. Freundlich, Over the Adsorption in Solution, *J. Phys. Chem.* 57 (1906) 385–471.
- [45] V. Tempkin, M.I. Pyzhev, Kinetics of ammonia synthesis on promoted iron catalyst, *Acta Phys. Chim. USSR.* 12 (1940) 327–356.
- [46] W.J. Weber, J.C. Morris, Kinetics of Adsorption on Carbon from Solution, *J. Sanit. Eng. Div.* 89 (1963) 31–59. <https://doi.org/10.1061/JSEDAI.0000430>.
- [47] S. Mopoung, P. Moonsri, W. Palas, S. Khumpai, Characterization and Properties of Activated Carbon Prepared from Tamarind Seeds by KOH Activation for Fe(III) Adsorption from Aqueous Solution, *Sci. World J.* 2015 (2015) 1–9. <https://doi.org/10.1155/2015/415961>.
- [48] D. Kosale, C. Thakur, V. Singh, Use of Jamun seed (*Syzyum Cumini*) biochar for removal of Fuchsin dye from aqueous solution, *J. Serbian Chem. Soc.* 88 (2023) 653–667. <https://doi.org/10.2298/JSC220830021K>.
- [49] Vibrational Spectra and Analysis of Trans – decahydronaphthalene, 1 (2010) 211–216.
- [50] K.S.W. Sing, Reporting physisorption data for gas/solid systems with special reference to the determination of surface area and porosity (Recommendations 1984), *Pure Appl. Chem.* 57 (1985) 603–619. <https://doi.org/10.1351/pac198557040603>.
- [51] L. Xu, J. Zhang, J. Ding, T. Liu, G. Shi, X. Li, W. Dang, Y. Cheng, R. Guo, Pore structure and fractal characteristics of different shale lithofacies in the dalong formation in the western area of the lower yangtze platform, *Minerals.* 10 (2020). <https://doi.org/10.3390/min10010072>.
- [52] F.R.-R. Matthias Thommes*, Katsumi Kaneko, Alexander V. Neimark, James P. Olivier, J.R. and K.S.W. Sing, Brunauer-Emmett-Teller (BET) surface area analysis, *Pure Appl. Chem.* 87 (2013) 1051–1069. [https://www.ru.ac.za/media/rhodesuniversity/content/nanotechnology/documents/BET Refilwe Matshitse.pdf](https://www.ru.ac.za/media/rhodesuniversity/content/nanotechnology/documents/BET%20Refilwe%20Matshitse.pdf).

- [53] K. Kinashi, Y. Kambe, M. Misaki, Y. Koshihara, K. Ishida, Y. Ueda, Synthesis, characterization, photo-induced alignment, and surface orientation of poly(9,9-dioctylfluorene-alt-azobenzene)s, *J. Polym. Sci. Part A Polym. Chem.* 50 (2012) 5107–5114. <https://doi.org/10.1002/pola.26338>.
- [54] M. Crespo-Alonso, V.M. Nurchi, R. Biesuz, G. Alberti, N. Spano, M.I. Pilo, G. Sanna, Biomass against emerging pollution in wastewater: Ability of cork for the removal of ofloxacin from aqueous solutions at different pH, *J. Environ. Chem. Eng.* 1 (2013) 1199–1204. <https://doi.org/10.1016/j.jece.2013.09.010>.
- [55] S.A. Hassan, F.J. Ali, Assessment of the Ofloxacin (Novecin) Adsorption from aqueous solutions by Two Agricultural Wastes, *Int. J. Adv. Sci. Tech. Res.* 2 (2014) 950–965.
- [56] D. Lin, B. Xing, Adsorption of phenolic compounds by carbon nanotubes: Role of aromaticity and substitution of hydroxyl groups, *Environ. Sci. Technol.* 42 (2008) 7254–7259. <https://doi.org/10.1021/es801297u>.
- [57] B. Peng, L. Chen, C. Que, K. Yang, F. Deng, X. Deng, G. Shi, G. Xu, M. Wu, Adsorption of Antibiotics on Graphene and Biochar in Aqueous Solutions Induced by π - π Interactions, *Sci. Rep.* 6 (2016) 1–10. <https://doi.org/10.1038/srep31920>.
- [58] H. Peng, B. Pan, M. Wu, Y. Liu, D. Zhang, B. Xing, Adsorption of ofloxacin and norfloxacin on carbon nanotubes: Hydrophobicity- and structure-controlled process, *J. Hazard. Mater.* 233–234 (2012) 89–96. <https://doi.org/10.1016/j.jhazmat.2012.06.058>.
- [59] H. Liu, W. Liu, J. Zhang, C. Zhang, L. Ren, Y. Li, Removal of cephalexin from aqueous solutions by original and Cu(II)/Fe(III) impregnated activated carbons developed from lotus stalks Kinetics and equilibrium studies, *J. Hazard. Mater.* 185 (2011) 1528–1535. <https://doi.org/10.1016/j.jhazmat.2010.10.081>.
- [60] M. Özacar, I.A. Şengil, Adsorption of metal complex dyes from aqueous solutions by pine sawdust, *Bioresour. Technol.* 96 (2005) 791–795. <https://doi.org/10.1016/j.biortech.2004.07.011>.
- [61] A.A.M. Daifullah, S.M. Yakout, S.A. Elreefy, Adsorption of fluoride in aqueous solutions using KMnO₄-modified activated carbon derived from steam pyrolysis of rice straw, *J. Hazard. Mater.* 147 (2007) 633–643. <https://doi.org/10.1016/j.jhazmat.2007.01.062>.
- [62] A. Chandrasekaran, C. Patra, S. Narayanasamy, S. Subbiah, Adsorptive removal of Ciprofloxacin and Amoxicillin from single and binary aqueous systems using acid-

- activated carbon from *Prosopis juliflora*, *Environ. Res.* 188 (2020) 109825.
<https://doi.org/10.1016/j.envres.2020.109825>.
- [63] N. Priyantha, L. Lim, M.K. Dahri, L.B.L. Lim, Dragon Fruit Skin as a Potential Low-Cost Biosorbent for the Removal of Manganese(II) Ions, *J. Appl. Sci. Environ. Sanit.* 8 (2013) 179–188. <https://www.researchgate.net/publication/261760667>.
- [64] R. Huang, B. Yang, Q. Liu, K. Ding, Removal of fluoride ions from aqueous solutions using protonated cross-linked chitosan particles, *J. Fluor. Chem.* 141 (2012) 29–34.
<https://doi.org/10.1016/j.jfluchem.2012.05.022>.
- [65] P. Tirkey, T. Bhattacharya, S. Chakraborty, Optimization of fluoride removal from aqueous solution using Jamun (*Syzygium cumini*) leaf ash, *Process Saf. Environ. Prot.* 115 (2018) 125–138. <https://doi.org/10.1016/j.psep.2017.10.022>.